CHAPTER 4: THE WATERBERG GROUP.

4.1: Introduction:

Within the study area, three Formations within the Waterberg Group have been identified (Appendix 1). These are the Setlaole Formation, Makgabeng Formation and the Mogalakwena Formation. Generally, the Setlaole Formation outcrops poorly, though a few isolated outcrops occur east of the Makgabeng Plateau (Figure 1.2). The Makgabeng Formation has excellent exposure at the type locality, the Makgabeng Plateau, though it is generally absent or poorly exposed in other parts of the study area. The Mogalakwena Formation can generally be found in locations throughout the area, though all Waterberg strata seem to be absent from the far north-western portion (Appendix 1).

4.2: Setlaole Formation:

The extent of outcrop of the Setlaole Formation is insufficient to establish the three-dimensional geometry, and so architectural elements for the Setlaole Formation could not be defined. The most northerly outcrop of the Setlaole Formation in the study area was found at 23°09.67'S; 29°03.50'E, where the unit consists of facies of planar and trough cross-bedded coarse sandstone and granulestone (Figure 4.1), with sub-rounded clasts and pebbles of quartz and quartzite. Many mesoscopic euhedral feldspar crystals and detrital micas are also present. Locally, small cobbles of foliated rocks (probably basement gneiss) can be found (Figure 4.2).

At 23°11.46'S; 29°01.79'E, the lithofacies are comparable to those outlined above, but are generally more mature. The lithology consists of coarse sandstone (granulestone occurs only locally), and there are no feldspars visible in hand specimens. Pebbles, where present, are all well-rounded and quartzitic (there are no feldspar-rich or foliated clasts). Palaeocurrents from both these localities are shown in Figure 4.3, and suggest that currents flowed towards the south.

The type locality for the Setlaole Formation is a low hill (Setlaole) at 23°21.60'S; 28°58.00'E, in the south-eastern corner of the study area, east of the Makgabeng plateau. Here, about 30-40m of sedimentary rocks is exposed on the eastern edge of the hill, which nonconformably overlies basement granite and amphibolite. The top part of the hill at Setlaole is underlain by a thick, sub-concordant diabase sill, which intrudes the Setlaole Formation, and which restricts the vertical extent of the outcrop of the Setlaole strata. At 23°20.36'S; 28°58.00'E, on the northern side of Setlaole, the nonconformity between the basement and the Setlaole Formation is exposed. The basal beds of the Setlaole Formation consist of a thin (c.15cm) quartz and granitic pebble conglomerate, with sub-angular pebbles having a maximum diameter of about 2.5-3cm (Figure 4.4). The pebble conglomerate is overlain by a 50cm-thick hard black mudrock (Figure 4.4). At this locality, less than 1m of Setlaole strata is exposed between the basement and the intruding diabase sill above.

Further to the south on Setlaole hill, at 23°20.90'S; 28°58.00'E, about 30m of Setlaole sedimentary rocks from higher in the Formation crop out. They consist of a coarse- and very coarse-grained sandstone and granulestone facies, with trough cross-beds (Figure 4.5). Sets are between 10 and 30cm in thickness, and preserved troughs are between 40 and 150cm wide. Rare quartz pebbles are present in the sandstones, and have a maximum diameter of 2-3cm (Figure 4.6). The rocks have a purplish colour, though are locally reduced to a pale cream colour, especially in beds composed of coarser sediment grains (Figure 4.6). The quartz grains in the sandstone are generally moderately to poorly sorted, with angular grains of low sphericity. Rare laminatae of medium to fine sandstone, which is moderately sorted, are also present. Palaeocurrent directions at this locality conform to the general southward direction recorded from Setlaole strata further north in the field area (Figure 4.7). Thin sections of the Setlaole Formation, taken from 23°16.33'S; 28°59.94'E show the feldspathic character of the unit in the north (Figure 4.8). Point counting (averaged from 300 points in 1 section) shows that this rock is comprised of 51% quartz, 29% matrix (=clay), 16% lithic fragments (=quartzite), 3% opaque minerals, and 1% feldspar. The rock is poorly sorted, and grains appear to be sub-angular and of low sphericity.

At 23°06.54'S; 28°49.38'E, 2km south east of My Darling (Appendix 1), a low hill is underlain by a white/pale cream pebbly granulestone (Figure 4.9), which bears considerable similarity to the facies observed at the Setlaole type locality (e.g. compare Figure 4.6 with Figure 4.9). Locally, quartz cobbles are also present, and reach a maximum diameter of 15-20cm. Coarse sandstone is interbedded with the pebbly granulestone, and is generally purple in colour. Pale coloured pebbly granulestone deposits are trough cross-bedded, though purple coarse sandstone exhibits planar bedding (Figure 4.10). Locally, clasts also consist of jasper and dark red-coloured coarse sandstone (Figure 4.11). Palaeocurrent directions measured from trough cross-beds suggest that transport was towards the south (an average trend of 197°), parallel with palaeocurrent directions measured from more southerly Setlaole strata (Figures 4.3 and 4.7). This outcrop has previously been mapped as belonging to the Blouberg Formation (Semaoko Grit Member; Jansen, 1976) and to the Soutpansberg Group (Callaghan and Brandl, 1991).

4.3: Makgabeng Formation:

Outcrop of the Makgabeng Formation is limited to an area in the south-eastern portion of the study area (Appendix 1). The most northerly outcrop of the Makgabeng Formation was recorded at 23°10.50'S; 28°52.70'E, about 4km south of the southern strand of the Melinda Fault Zone. Outcrop quality of the Makgabeng Formation is generally good to the south of this area, especially at the type locality, the Makgabeng plateau (Figure 1.2). In the south-western part of the study area, the Makgabeng Formation is overlain and largely obscured by the Mogalakwena Formation, and consequently the western extent of the Formation within the study area cannot be determined, though the most westerly outcrop of the Makgabeng Formation was recorded in the banks of the deeply incised Mogalakwena River at Steilloopbrug (23°25.94'S; 28°37.20'E), where the river has cut down through the thin layer of overlying basal Mogalakwena Formation conglomerate, to expose the upper strata of the Makgabeng Formation. It thus seems likely that the Makgabeng Formation underlies the Mogalakwena Formation throughout the study area.

Within the type locality, a vertical section of the Formation is exposed in cliffs on the northern edge of the Makgabeng plateau. The plateau area itself exhibits three-dimensional outcrops of the upper part of the Formation. In the plateau area, the Makgabeng Formation is between 300 and 400m thick. A borehole drilled through the Mogalakwena Formation 4km south-west of Steilloopbrug (approximately 23°28'S; 28°36'E) intersected 570m of Makgabeng Formation strata, locally intruded by diabase sills (Van der Neut, 1994). The underlying Setlaole Formation was intersected 639m below the surface. The borehole core was also logged during the present study, and a summary of this log is shown in Figure 4.12. As previous workers (Meinster and Tickell, 1975; Callaghan, 1987; Callaghan et al., 1991; Eriksson et al., 2000) are unanimous in their interpretation that the strata of the Makgabeng Formation were deposited in an aeolian palaeoenvironment (Section 1.4.2), a brief discussion of aeolian bounding surfaces is pertinent. This study will focus on a consideration of architectural elements and detailed interpretation of both aeolian and aqueous processes within the Makgabeng palaeo-desert.

Generally, the Makgabeng Formation is preserved as inclined foresets (Section 4.3.3.1), though rare bedding surfaces show horizontal inclination, indicating that the Makgabeng Formation is relatively tectonically undisturbed. The rocks of the Makgabeng Formation are pale coloured red-beds, though these are often reduced along certain foreset and bedding planes and within spherical reduction spots. Reduced areas are pale cream in colour.

4.3.1: Bounding surfaces in aeolian sediments and sedimentary rocks:

The scheme of architectural element analysis (Miall, 1985), developed initially for classification of fluvial sediments cannot be readily applied to aeolian deposits, though previous workers (e.g. Brookfield, 1977; Kocurek, 1988; Blakey *et al.*, 1996) have stressed the importance of the identification of bounding surfaces within aeolian sediments. Brookfield (1977) classified a three-stage hierarchy of bounding surfaces within an aeolian environment. First-order surfaces (largest scale) are flat-lying bedding

surfaces, which are attributed to the passage of draas (large dunes with smaller parasitic dunes migrating on the stoss and lee sides), across an inter-dune area. Second-order surfaces (which may be cut by first-order surfaces) bound individual dunes and are attributed to the migration of dunes across draas (they are, essentially, a cross-bed set boundary; Figure 4.13). Third-order surfaces are 'reactivation surfaces' (McKee, 1966) within an individual dune foreset, caused by temporary changes in transport (i.e. wind) direction, leading to fluctuation in dip direction of the dune foresets (Brookfield, 1977). Third-order surfaces may be cut by first- and second-order surfaces (Figure 4.14a). The three orders of surfaces outlined above may all be climbing surfaces, i.e. the features can move upwards relative to a horizontal depositional surface (Figure 4.14b), due to the prograding-upwards nature of migrating sand dunes (Brookfield, 1977).

Kocurek (1988) identified yet another surface, of lower order than a first-order surface, and which does not climb (i.e. the surface is generally horizontal, apart from localised relict dune topography) formed by a major hiatus in erg (sand sea) deposition (Figure 4.14b). Such surfaces are termed 'super surfaces' and the hiatus in sedimentation can be caused by *climatic change*, *tectonic* and *sea level change* or by the *migration of ergs* (Kocurek, 1988) across an area to a site more favourable for deposition. *Climatic change* can either promote or degrade an aeolian environment by controlling surface vegetation (not applicable to Proterozoic ergs), controlling the input of sand into an erg by fluvial transport (i.e. rainwater runoff) and by changes in wind direction and velocity. *Tectonic* control over super surface formation is influential by means of a greater sediment supply from uplifted source areas (provided, of course, that the tectonically uplifted area is upwind of the erg and weathers to provide grains of suitable size for deflation). It is possible, however that wind direction may be modified by topography, and thus there is an additional, indirect tectonic control over wind direction. Eustatic fall in *sea level* enhances continental freeboard, and promotes erosion of this high-lying continental region, thus maximizing sediment supply. A sea level rise can create intervening water bodies within an erg, which act as barriers to aeolian sedimentation. The *migration of ergs* into, or away from a particular area is controlled by whether the area is suitable for deposition or deflation (i.e. wind erosion). Generally, areas which are sites of deposition

are areas of deceleration of wind speed, such as those caused by wind blowing over a topographical basin, which allows the sediment-laden air to expand vertically, decelerate and become supersaturated with sand, which is therefore deposited from suspension. Erg margins therefore commonly follow topographic contours (Kocurek, 1988), and thus the margins of highland areas act as boundaries for erg deposition. Deceleration may also occur in areas where winds with different directions converge, accounting for an overall drop in wind velocity (Kocurek, 1988). Similarly, areas which have accelerating or diverging winds passing over them (e.g. winds blowing up highland areas, or where wind is forced through a topographical constriction) are undersaturated with sand, and become deflated (Bagnold, 1954; Kocurek, 1988).

Thus, a hiatus in deposition, due to a shift in conditions favourable for deposition to those favourable for deflation, caused by any or several of the reasons outlined above, will result in the creation of a super surface across the erg. The level in the erg at which a super surface develops is often controlled by deflation down to a horizontal surface within the erg at which deflation is impeded. Commonly, such surfaces represent the palaeo-water table (wet sand cannot be wind-blown), an armoured lag deposit within the erg (a layer of rocks too large to be moved by aeolian transport), or the development of a vegetated layer (again, not applicable to Proterozoic aeolian deposits, although microbial mats may have played a role). Alternatively, deflation could simply be stopped by renewed sedimentation (e.g. the migration of a subsequent erg over the deflated erg, or by a change in environment, leading to overlying alluvial or marine deposits; Kocurek, 1988).

Clues as to the cause of the development of the super surface often remain in the geological record. Super surfaces developed at a water table may contain evidence for evaporites, polygonal desiccation cracks and enhanced cementation of sand (i.e. playa lake deposits). Those developed due to a climatic change to more humid conditions show evidence for rapid stabilization of dunes by vegetation, thus leading to relict dune topography, plant roots and soil horizons along the super surface. Importantly these diagnostic features would not be expected in aeolian deposits earlier than the

Phanerozoic. Super surfaces caused by lag deposits are readily identifiable by the presence of the lag at the surface, and those caused by erg migration tend to produce a super surface with planar palaeotopography (no increase in rainfall means vegetation cannot stabilise the dunes). Super surfaces which are drowned by later sediments (i.e. if sedimentation is renewed before deflation down to the water table or a lag deposit) can be identified by the fact that they cut first-order surfaces (in the case of resumed aeolian sedimentation), or by the presence of contrasting sediments (in the case of the onset of marine or fluvial sedimentation) (Kocurek, 1988).

The four-order hierarchy of surfaces within aeolian sediments therefore gives an architectural framework within which an aeolian deposit can be considered, that is comparable to the architectural element scheme applied to fluvial sediments by Miall (1985). In particular the identification of a super surface is important as it gives clues to the causes of development of the surface and, as such, is an important tool for the interpretation of syn-depositional conditions (such as tectonic, eustatic and palaeoclimatic change). Additionally, identification of a super surface acts as a powerful means of correlation between outcrops.

4.3.2: Bounding surfaces present in the Makgabeng Formation:

High-order (i.e. second- and third-order) surfaces are present in most outcrops of the Makgabeng Formation. Figure 4.13 shows a second-order surface developed between two dunes, which reflects deposition in two opposing wind directions. Figure 4.14a shows a third-order surface (a reactivation surface; McKee, 1966) which similarly developed as a result of fluctuating wind direction, though in this case, the angle between the earlier and later wind directions was slight, and did not lead to total destruction of the earlier dune.

First-order surfaces could not be identified within the Makgabeng Formation, though two examples of super surfaces could be identified. The first consists of laterally extensive playa lake deposits, which can be traced horizontally for up to 5km at the northern edge of the Makgabeng Plateau at 23°13.60'S; 28°52.80'E (Section 4.3.3.3).

The second super surface identified marks the contact between the Makgabeng Formation and the overlying Mogalakwena Formation. Regionally, the conglomerates and sandstones of the latter are thought to have a conformable relationship with the aeolian deposits beneath (Callaghan *et al.*, 1991). The contact between the two formations, shown in Figure 4.15, is clearly sharp, and can be mapped for several hundred metres as exhibiting little palaeotopography at the contact. Topmost aeolian dunes in the Makgabeng Formation were generally largely eroded prior to the onset of fluvial Mogalakwena sedimentation (Figure 4.15). Such a non-climbing architecture for these topmost palaeo-dunes therefore clearly represents a super surface.

4.3.3: Facies present in the Makgabeng Formation:

The sedimentary rocks of the Makgabeng Formation, bound by the hierarchy of surfaces outlined above, are composed of five facies associations; (1) large-scale trough and planar cross-bedded sandstone, (2) horizontally bedded and rippled mudstone and sandstone, (3) horizontally and cross-bedded sandstone and mudstone, (4) massive sandstones, and (5) planar bedded and trough cross-bedded pebbly sandstone.

4.3.3.1: Large-scale trough and planar cross-bedded sandstone facies association:

This facies association consists dominantly of inversely-graded foresets of laminated, well sorted, well rounded, fine- to medium-grained, locally rippled sandstone, with minor, thin wedge-shaped strata (Simpson *et al.*, 1999). The inversely graded sandstone occurs in laminations between 2 and 10mm thick (Figure 4.16), though the average thickness of each lamina is around 5mm. Each lamination shows inverse grading from fine-grained sandstone at the lower surface of the lamination to medium-grained sandstone on the upper surface of the lamination, and consists of well-sorted quartz arenites (Figure 4.16). The diagnostic inverse-grading of strata can often only be recognised in the field by examination with a hand lens of exposure faces which have developed at a shallow angle to the lamination plane. Thus a very oblique exposure

section through a thin lamination provides a surface on which changes in grading between fine- and medium-grade sandstones within the lamination can be identified more easily. Asymmetric ripplemarks are rarely preserved in association with low-angled, inversely-graded strata (Figure 4.17). Ripple wavelength averages 7.5cm, and they have an average amplitude of about 3mm. Ripple index (wavelength/amplitude) averages 25, and ripple symmetry index (crest to trough distance/wavelength) averages 0.3.

The inclination of inversely-graded cross-strata varies from horizontal to a high angle of inclination (reaching a maximum preserved angle of about 25-30°) (Figure 4.18). The thin wedge-shaped strata occurring between the inversely-graded foresets taper in the down-dip direction (Figure 4.19), and are generally found in association with high-angled inversely-graded cross-strata, and usually dip in excess of 20°. They are also composed of fine- to medium-grained laminated arenites, though they contain no evidence for internal grading (Figure 4.19). In plan view, wedge-shaped strata extend for between 50cm and 3m across the foresets, and may be up to 30cm thick (Simpson *et al.*, under review). The lower contacts of wedge-shaped sets with underlying inversely-graded strata are irregular to sharp.

The inversely-graded strata and wedge-shaped strata can be found together in both planar and trough cross-bedded sets in the Makgabeng Formation. Large-scale mapping of foresets on the Makgabeng plateau was undertaken by use of plane table and open sighted alidade. This map is shown in Figure 4.20, and identifies a combination of foresets which have a consistent strike (i.e. planar cross-bedding), and foresets which have a variable strike, so that dip-directions converge (i.e. trough cross-bedding), and which are arcuate in plan view. The average dip direction of foresets can be used to determine palaeowind directions. Callaghan (1987) determined an average palaeowind direction of 226° based on foreset directions in the Makgabeng Formation. Similarly, foreset directions recorded in the study area (insert in Figure 4.20) suggest a palaeowind direction towards, on average, 215°.

Preserved planar cross-bedded sets vary in set thickness between 1.5 and 10m, and the strike of planar foresets can be traced for over 150m without appreciable change in strike orientation (Simpson *et al.*, under review). In the down dip direction, foresets can be traced for up to 400m, with little change in the foreset dip angle at a consistent height above the lower set boundary (Simpson *et al.*, under review). Dip angles of foresets vary between horizontal and 28°. Preserved trough cross-bedded sets are between 1 and 6m thick, and can be traced laterally for up to 70m (Simpson *et al.*, under review). Angles of the dip of foresets vary from horizontal to 22° at the set top. Sets of both planar and trough cross-bedded strata are bounded by 2nd order surfaces, and locally contain 3rd order surfaces.

Generally, within the Makgabeng Formation in exposures on the Makgabeng Plateau, it was found that trough cross-bedded sets are dominant in the lowermost half of the Formation, and are then superseded by planar cross-bedded sets towards the top. However, in the uppermost part of the Formation, in common association with the presence of the massive sandstone facies association (Section 4.3.3.4) there is a return to the predominance of trough cross-beds.

4.3.3.2: Horizontally bedded and rippled mudrock and sandstone facies association:

The data presented here were recorded in a cliff section on the northern edge of the Makgabeng plateau at 23°13.60'S; 28°52.80'E, though evidence for this facies association was also found in the core from the bore hole drilled 4km south-west of Steilloopbrug (approximately 23°28'S; 28°36'E; Figure 4.12), and in the top most 2m of the Makgabeng Formation at Steilloopbrug (23°25.94'S; 28°37.20'E).

Four lenses of laminated mudstone and sandstone beds were found on the north of the plateau, which extend laterally for up to 100m, before pinching out or being truncated by large-scale trough cross-bed deposits. The lenticular strata are between 40 and 110cm thick (Eriksson *et al.*, 2000), and together occupy approximately 5m in thickness within the Magkabeng succession exposed within the cliff face. The lower surface of the facies

association is conformable with the upper bounding surfaces of horizontally inclined strata of the large-scale cross-bedded facies association beneath. The beds of this lenticular facies association are internally comprised of facies of massive sandstone, wave, combined flow, current and wind rippled sandstones and mudrocks (Figure 4.21 and 4.22) (Eriksson *et al.*, 2000). Additional minor structures also present locally are adhesion structures, mudcracks (Figure 4.22), rolled-up mud laminations (Figures 4.23 and 4.24), rainspots and evaporite casts, probably of gypsum crystals (Figure 4.25) (Simpson *et al.*, 1999; Eriksson *et al.*, 2000). These structures are arranged with massive, horizontally stratified and current rippled sandstones at the base, followed by wave and combined flow ripples above. In the upper most part of the beds, wind-rippled sandstone, adhesion warts, desiccation cracks and evaporite casts are found (Simpson *et al.*, 1999).

With a general absence of preserved bedding planes in the large-scale trough and planar cross-bedded facies (mostly only inclined foresets are well preserved, with fewer bounding surfaces), horizontally bedded deposits of this facies association offer rare evidence for the direction of tectonic dip of the Makgabeng Formation. Generally, lenticular occurrences of the horizontally bedded and rippled mudrock and sandstone facies association in the Makgabeng Formation retain their horizontal dip (and rarely have a dip in excess of 5°), indicating a general lack of deformation within the Makgabeng Formation.

The rolled-up mud laminations found within this facies association consist of red-coloured silty mudstone laminations between 1 and 2mm thick (Figures 4.23 and 4.24). The laminations are curled into cylindrical, cigar-shaped structures, so that the original upper surface of the lamination is facing towards the centre (Eriksson *et al.*, 2000). The roll-up structures are up to 5cm in length, 2-3cm wide and consist of up to two or three concentric layers (i.e. more than 720° of curvature on the upper surface of the lamination). The long axes of these structures are orientated approximately parallel to each other (Eriksson *et al.*, 2000). The structures show evidence for having been slightly flattened perpendicular to the bedding plane, and are now elliptical in shape. Several

other mudchips, which only show slight curling, are also associated with the roll-up structures (Eriksson *et al.*, 2000).

4.3.3.3: Rippled and cross-bedded sandstone facies association:

This facies association is also observed in the vertical cliff on the northern edge of the Makgabeng plateau at 23°13.60'S; 28°52.80'E, a few metres above the horizontally bedded, rippled mudrock and sandstone facies association previously described, and can be traced laterally for up to 5km, and reaches a maximum thickness of about 30m. This cross-bedded sandstone facies association contains a basal decimetre–thick mudrock, though it is generally sandy for the majority of the sequence above. The sandstone facies above contains the following structures; asymmetric ripples (both strongly and weakly asymmetric), symmetrical ripples, inversely graded laminations in sandstone (identical to that described in Section 4.3.3.1) and, more rarely, massive sandstone and horizontally laminated sandstone (Simpson *et al.*, under review). The beds are arranged in vertical sequences which fine and thin upwards, from medium- to fine-grained sandstone or mudrocks. The structures are commonly arranged from bottom to top in the following manner: strongly assymmetrical ripples, inversely graded laminations, slightly asymmetrical ripples, asymmetrical ripples, inversely graded laminations, symmetrical ripples, inversely graded laminations, symmetrical ripples, massive sandstones, symmetrical ripples, inversely graded laminations, and massive sandstone (Simpson *et al.*, under review).

Thin lenses of large-scale, cross-bedded facies are also present, though they are not laterally continuous. Generally these occurrences of the large-scale, cross-bedded facies association exhibit low to horizontal angles of dip.

In addition to the structures previously described, the top surfaces of the thinning and fining upwards sequences contain small pits, less than 3mm deep. The pits are filled with sandstone, mudstone or siltstone from the overlying bed. The sand grains around the pits

are less well sorted than the surrounding beds, and the area of 2-3mm radius around the pit is a zone of preferential quartz cementation (Simpson *et al.*, under review).

Samples of this facies association taken from the borehole core were analysed by X-ray diffraction, which showed trace amounts of anhydrite and lesser amounts of gypsum present.

4.3.3.4: Massive sandstone facies asscociation:

This facies association is found generally in the upper half of the Makgabeng Formation, and is especially well exposed in good three-dimensional outcrops across the top of the Makgabeng plateau area, beneath the contact with the Mogalakwena Formation. This trend is also shown in the bore hole log (Figure 4.12) which shows that occurrences of this facies association are less common in the lower most half of the Formation. Generally the facies association occurs as planar-based, lenticular bodies, between 5cm and 6m in thickness, and between 1 and 50m in lateral extent in any one direction, and which generally contain no internal structures (Figure 4.26). In thin section, rocks of this facies association appear petrographically identical to those of the large-scale cross bedded sandstone facies association. The lenticular massive sandstone bodies tend to overlie horizontal to low-angle large-scale, cross-bedded facies, and can locally be traced up the foreset, where massive beds may onlap onto 3rd order reactivation surfaces (Figure 4.27). Locally, often in association with medium to high angles of inclination of cross-bed foresets (up to 26^{o}), the geometry of the massive sandstones is channelised, rather than lenticular (Figure 4.28). Bases of the channelised massive sandstones are sharp and erosional into the underlying foresets (4.29). The edges of the channels are generally steep, vertical and rarely overhanging (Figure 4.28). Preserved channel forms may be up to 2m deep and 4m wide, though most are generally smaller. The long-axis of the channel is usually parallel or slightly oblique to the dip-direction of the large-scale foreset that it cuts. Down-dip, channels can be observed to expand into the massive lenticular bodies previously described. As the channel form spreads, the relationship with the substrate changes from channelised and often erosional to either conformable or onlapping, and the

massive body is also likely to thicken. One measured channel axis had an azimuth of 290°, and spread horizontally outwards towards the bottom of the palaeo-dune slip face to form a lenticular body with margins trending 200° to 020°, showing that the lenticular sandstone body is lobate-shaped. Rarely, channels and lenticular bodies can be observed to contain thin layers of wind ripple laminae between two successive massive sands, reflecting two distinct phases of infill, separated by a dry, windy period. In places a few rotated blocks of laminated, large-scale, cross-bedded facies, of between 10 and 50cm diameter, could be observed within massive sandstone bodies. Additionally, at one locality, large-scale cross-beds were over-folded beneath a channelised massive sandstone.

Locally, in close proximity to areas exhibiting massive sandstones, steeply dipping cross-strata of the large-scale cross-bedded sandstone facies association could be seen to have undergone soft sedimentary deformation (Figure 4.30). The deformation appears to be related to slumping, with slumps verging in a down-dip direction. Although the laminations of cross-bedded strata are strongly folded to accommodate the slump, laminae are not destroyed (Figure 4.30).

The upper surfaces of massive sandstones may contain a variety of features including adhesion warts, wind ripple strata, shallow concave-up depressions containing inversely-graded wind-ripple strata, horizontally laminated sandstones with parting lineations, ball and pillow structures, convolute structures and rare desiccation cracks.

4.3.3.5: Pebbly sandstone facies association:

This facies association was only identified locally in the upper most 50m of the Makgabeng Formation. The outcrop is located around 23°16.07'S; 28°52.42'E, and the occurrence of the facies association is about 750m long, 500m wide, and has a stratigraphic thickness of about 30m. The long axis of the outcrop trends approximately N-S. To the south, the facies association erosively overlies large-scale trough cross-bedded facies, and is, in turn, overlain by trough cross-bedded facies to the north. The

eastern and western margins of the exposure show that pebbly sandstones interfinger with the large-scale trough cross-bedded facies. The pebbly sandstone facies association consists of medium- to coarse-grained, locally planar-bedded sandstones, which comprise well-rounded sand grains of generally high sphericity. Sand grains appear well-sorted, and are about 500μm in diameter, though lithic fragments (quartzite) up to 3mm diameter may also be present rarely. Interstitial areas within the coarse sandstone are locally filled with jasper or opaque minerals. The strata of the pebbly sandstone facies association can be easily recognised as it is generally massive compared to the thinly laminated sandstone of the large-scale, cross-bedded facies association (Figure 4.31). The pebbly sandstone facies association of the Makgabeng Formation is also readily identifiable from large-scale, cross-bedded and massive facies associations by the presence of isolated quartz pebbles (Figure 4.32). Individual beds of the pebbly sandstones are about 15cm-1m thick, and are locally normally graded. The bases of the beds may contain isolated quartz or quartzite pebbles, typically with a diameter between 2 and 7cm, within a matrix of coarse-grade sand grains. Towards the top of the bed, no larger clasts occur, and medium-grained sandstone is present. Trough and planar cross-bedding (Figure 4.33), preserved channels and parting lineation on planar bedding surfaces (Figure 4.34) are subordinate characteristics of this facies association, which serve to indicate palaeocurrent direction. Preserved channel forms are typically around 5-11m wide and 50-70cm deep, and are generally sandstone-filled, and free from larger clasts. The rose diagram in Figure 4.35 shows that the transport direction was generally towards the south.

Deeply incised, steep-sided channels generally mark the contact between the pebbly sandstone and the large-scale cross-bedded facies association (Figure 4.31). Such channeling suggests that the cross-bedded facies had not lithified at the time of deposition of the pebbly sandstone, and hence were more easily eroded. Locally, pebbly sandstone facies can be observed to lie directly over very steeply inclined foresets (29-30°) of the large-scale trough cross-beds (Figure 4.36).

4.4: Mogalakwena Formation:

In this section, the Mogalakwena Formation will be considered from two areas: the strata which outcrop south of the southern strand of the Melinda Fault, and the Mogalakwena strata which outcrop north of the southern strand of the Melinda Fault (Appendix 1). These latter rocks have previously been considered as a part of the Blouberg Formation (Mositone Conglomerate, Varedig Sandstone and Semaoko Grit members; Jansen, 1976; Section 1.3.1) and of the pre-Blouberg Lebu Complex (Meinster, 1977; Section 1.3.2), or as part of the Soutpansberg Group (Brandl, 1991; Callaghan and Brandl, 1991; Barker *et al.*, in press; Section 1.3.3).

4.4.1: Mogalakwena strata south of the southern strand of the Melinda Fault:

4.4.1.1: Eastern part of the study area:

The strata of the Mogalakwena Formation south of the southern strand of the Melinda Fault are generally horizontal to sub-horizontal, and only rarely dip at angles in excess of 30° (Appendix 1). Generally, the outcrops are large and provide good three-dimensional exposures (the lithology does not support thick soils and dense vegetation), and commonly the Mogalakwena Formation outcrops as isolated, steep-sided mesas (Figure 4.37). Such outcrops allow for the determination of the large-scale three-dimensional geometry for the identification of architectural elements (Miall, 1985) more readily than other inferred fluvial sedimentary rocks previously discussed.

Generally the elements consist of interbedded sheet-like structures of either coarse sandstone and granulestone or conglomerate (Figures 4.37 and 4.38), which correlate with element CHS (major sandstone sheet) of Miall (1985; 1996; Table 3.1). Sheets are generally 50cm to 1m thick, and hundreds of metres across in lateral extent. Locally these sheets are intersected and cut by large conglomerate-filled channel forms (element CHR of Miall, 1985; 1996; Table 3.1), up to 20-30m in cross section, and 2-5m in depth (Figure 4.39). Where channels are exposed within a steep side of a mesa, the trend of the

palaeocurrent can be determined by the identification of the channel on the opposing side of an adjacent mesa.

Sheet-like elements are comprised of both matrix-supported conglomerate and medium- and coarse-grained sandstone and granulestone. Conglomeratic sheets are generally massive, and internal primary structures (e.g. bedding and cross-bedding) tend not to be present. Figure 4.40 shows rare imbrication of quartz and quartzitic cobbles, which indicates opposing palaeocurrent directions from the trough cross-bedded coarse sandstone facies above.

The conglomerates are generally matrix-supported (Gmm; Table 3.1), with a matrix of coarse sand and granule sized grains, with some opaque minerals also present. Cobbles and pebbles tend to be well rounded and spherical, so imbrication is only rarely detectable (Figure 4.41). Cobbles are mainly composed of quartz, quartzite, green quartz (fuchsite stain) and, locally, pebbles of Banded Iron Formation (B.I.F.) (Figure 4.42).

In sandstone and granulestone sheets, trough cross-bedding (St; Table 3.1) is the only common internal sedimentary structure, with set thickness commonly between 30 and 50 cm (Figure 4.43) and cobble-sized clasts are rare. Grain size is variable from 500μm (medium- to coarse-grained sand) to 3-4mm (granules). Generally granule-sized grains appear most common in thin sections from samples taken from the non-conglomeratic sheets, and are composed of quartz and quartzitic lithic fragments (Figure 4.44). Large granule-sized grains are poorly sorted, angular and of low sphericity, whereas rare patches of medium- to coarse-grained sandstone matrix have grains that are well sorted, sub-rounded and of medium sphericity (Figure 4.45). An average of 500 point counts taken from one thin sections sampled from sandy sheets show that the finer components of these Mogalakwena sedimentary rocks are composed of 40% quartz, 39% matrix (intergranular material) and 21% lithic fragments. A photomicrograph of this rock is also shown in Figure 5.18.

In order to establish variation between interbedded conglomeratic and granulestone sheet-like elements within the Mogalakwena Formation, a systematic survey was made, using a $1m^2$ grid (methodology outlined in Section 1.6.1). Variation in the composition and size of conglomerate clasts and also how these parameters vary with stratigraphic height and distance from the Melinda Fault can also be determined using this method. Granulestone and coarse sandstone beds are indicated by a paucity of recorded conglomerate-sized clasts. The measurements were taken from the following locations: From north to south: 23°11.23'S; 28°52.44'E on Blackhill 317LR; 23°11.52'S; 28°52.28'E at Tsolametse (northern slope); 23°11.66'S; 28°52.21'E at Tsolametse (southern slope); 23°13.60'S; 28°51.65'E at the east side of Sadu, on Gallashiels 316LR and 23°16.20'S; 28°50.50'E, at Masebe, on Montblanc 328LR (Figure 4.46). These five locations are located on a line trending approximately perpendicular to the strike of the Melinda Fault, and lie south of the southern strand (Figure 4.46). Data are presented in Appendix 2. This style of survey was carried out in preference to the calculation of palaeohydraulic parameters, used for the Blouberg Formation (Section 3.5) on account of the paucity of recorded channel forms in the Mogalakwena Formation. Whilst paleaohydraulic parameters could have been calculated from the trough cross-bedded granulestone sheets, such calculations would not have encompassed the palaeohydraological parameters relating to the ubiquitous conglomeratic sheets, and thus would give little indication of the true conditions during deposition of the Mogalakwena Formation.

Measurements of the percentage of pebble- to boulder-sized clasts in the conglomerate (i.e. those larger than about 1cm) relative to matrix, in the basal 90m of the Mogalakwena Formation at these five locations are shown in Figure 4.47. Figure 4.47 shows the overall cyclical nature of the lower Mogalakwena sediments, with peaks corresponding to conglomeratic beds, and troughs (caused by a paucity of larger-sized clasts) representing more sandy beds. Superimposed on this generally cyclical pattern of sedimentation, is an overall trend that the percentage of clasts within the matrix decreases upwards, with a sharp decrease in the percentage of larger-sized clasts about 30m above the unconformity with the Makgabeng Formation.

A general trend that clast frequency decreases towards the south is also evident from these data. Average values for clast frequency from each of the five localities (calculated by the sum of all percentages for each m^2 at each locality, divided by the height in metres of the recorded section) cannot be used as an indicator of relative clast frequency between each locality, as the clast frequency is largely a reflection of stratigraphic height (Figure 4.47).

Therefore, as the stratigraphic height from which data were collected varies between each locality, average values would rather reflect the stratigraphic height from which they were recorded, and not necessarily reflect a north-south trend. (e.g. the northern slope of the Tsolametse locality only contains data from the generally conglomeratic basal 15m of the Formation, so average values would be higher than the Masebe locality, where 67m of less-conglomeratic upper Mogalakwena strata was recorded). Therefore, to avoid such error, regional comparisons between localities should only be made from data recorded at the same stratigraphic height. Figure 4.47 shows that between the stratigraphic heights of 0m and 13m, data are recorded from four out of the five localities (only the Masebe locality is missing data from this stratigraphic height). Therefore this provides the best stratigraphic interval from which comparisons between localities can be made. Average values of clast percentages from within this13m interval are shown in Figure 4.48, which shows a slight overall decrease in clast frequency towards the south, though the trend is not clear.

In addition to the percentage of clasts and matrix within any particular m^2 of exposed strata, the length of the intermediate axis of the largest clast within that m^2 was also measured (Appendix 2). These collected data are presented in Figure 4.49, and again show the cyclical nature of the coarseness of the beds, and that generally clast size varies inversely with stratigraphic height. This relationship is most noticeable in the data from the southern slope of Tsolametse. Similarly, by comparison of clast size from between 0 and 13m height in the stratigraphy, there is also an apparent relationship, which shows that clast size generally decreases from north to south (Figure 4.50).

Multiplication of clast percentage and the length of the intermediate axis of the largest clast within that m^2, gives an overall index of the coarseness of that particular height in the stratigraphy. Highly conglomeratic beds with large clasts have a high resultant product, whereas more sandy beds with fewer, smaller clasts have a low product. Thus any trends of fining upwards and southwards can be exacerbated. Figure 4.51 shows how the overall coarseness of beds varies with stratigraphic height in the Mogalakwena Formation. Figure 4.52 shows the general coarseness of beds recorded in strata from the 0-13m interval. Although there is a general drop in coarseness of beds towards the south, again the southwards-fining trend shown in Figure 4.52 is not strong.

It is important to note that in many instances, the stratigraphic height within the Formation (i.e. the height above the unconformity with the Makgabeng Formation) had to be estimated (e.g. the basal part of the succession was hidden beneath talus at the Masebe location). Additionally the cyclical nature of the strata makes correlations between individual conglomeratic beds difficult between neighbouring locations. It is therefore possible that correlations in stratigraphic height made between localities within the Mogalakwena Formation are inaccurate. As the upper and lower boundaries of each m^2 interval measured do not necessarily coincide with a facies boundary plane, often each m^2 would contain parameters measured from both a sandy and a conglomeratic facies. This has the effect of smoothing the curves plotted in Figures 4.47, 4.49 and 4.51, as more average values are recorded.

Within these five locations the composition of the clasts per m^2 was recorded. Clasts which were recorded are vein quartz, quartzite, with rare clasts of fuchsitic quartz and B.I.F (Appendix 2). Figure 4.53 shows that both quartz and quartzite decline upwards in the stratigraphy (as clast frequency decreases; Figure 4.47). The presence of B.I.F. clasts in the Mogalakwena conglomerate seems to be strongly controlled by stratigraphic height within the Formation (Figure 4.53), with B.I.F. clasts occurring only rarely at stratigraphic heights greater than 20m. Figure 4.54 shows the variability of average percentages of clasts present for each location between the 0 and 13m interval. Percentages of vein quartz clasts are high in the north (an average of 10%), and generally

decline towards the south, whereas percentages of quartzite fragments seem to vary less systematically (Figure 4.54). Due to the lack of outcrop of the basal 20m at the Masebe location, it is difficult to assess the lateral variation in B.I.F. clast presence, though thin basal conglomerates in the Steilloopbrug area (23°25.94'S; 28°37.20'E and at 23°15.38'S; 28°42.39'E) also contain B.I.F. clasts. Thus it seems that the presence of B.I.F. clasts is controlled stratigraphically, rather than by distance southwards from the Melinda Fault.

In summary, the general sedimentary characteristic of the Mogalakwena Formation in the eastern part of the study area embodies interbedded trough cross-bedded coarse sandstones and massive matrix-supported conglomerate. These facies are found as sheet-like architectural elements with rare conglomeratic channel elements. There is a general trend of cyclicity between sandstone and conglomerate beds, with overall trends of upwards-fining and a weaker trend of southward-fining away from the area of the southern strand of the Melinda Fault.

Palaeocurrent directions for the Mogalakwena Formation south of the Melinda Fault can be derived from trough cross-bedding foreset directions in the sand sheets. Palaeocurrent directions from the imbrication of clasts in the conglomeratic sheets could not be readily determined due to the general roundness of clasts. Palaeocurrent directions recorded for these strata are shown in Figure 4.55, which shows a unimodal palaeocurrent direction towards the S.W. (c.246°).

4.4.1.2: Western part of the study area:

The stratigraphic patterns described above for the Mogalakwena Formation in the eastern part of the study area are only partially applicable to the western area south of the southern strand of the Melinda Fault. The general sheet-like architecture with rare channels (elements CHS and CHR respectively; Miall, 1985; 1988; Table 3.1) is similar to that identified in the east (Figure 4.56), though there is a marked difference in the distribution of conglomerate-sized clasts. The fining-upwards pattern identified in the

Mogalakwena Formation conglomerates in the eastern part of the field area is still present in the west, although the cobble-sized clasts in the western conglomerates are generally found only in the basal 10 or 15m of the Mogalakwena strata above the Makgabeng Formation, and thus are restricted to a considerably smaller portion of the stratigraphy. Field observations suggest that the composition of the clasts is identical to those in the east (quartz and quartzite, with rare B.I.F. and fuchsitic quartz clasts). In the basal 10-15m of the Mogalakwena Formation, conglomerate sheets are 30-50cm thick, and are interbedded with coarse-grained sandstone sheets. Clasts have a maximum diameter of 10cm, which is smaller in size than those measured at this stratigraphic height in the east. Conglomerates are commonly located in channel elements (Figure 4.57) in this basal portion of the Mogalakwena stratigraphy. Upwards, the frequency and thickness of conglomeratic sheets decreases (sheets may only be one clast thick by about 20m height in the stratigraphy), and coarse granulestone and sandstone sheets become dominant.

Above this basal 15m, Mogalakwena strata only rarely contain pebble and cobble-sized clasts, and facies of coarse-, very coarse-grained sandstone and locally gravel-sized clasts are prevalent within each sheet-like architectural element. The presence of channel elements also decreases upwards with the increasing rarity of conglomerates.

Trough cross-bed set thickness in the sandstone sheets is generally smaller in these westerly outcrops of Mogalakwena strata, and is often between 10 and 15cm (Figure 4.58). Heavy mineral concentrations on foresets are diagnostic, and serve to enhance the appearance of foresets (Figure 4.58). This lithofacies is comparable with that of the Sandriviersberg Formation at the southern edge of the Main Waterberg basin, which grades laterally into the Mogalakwena Formation towards the N.E. (Figure 1.6). Figure 4.59 is taken at 24°20.00'S; 28°33.50'E at the south-eastern corner of the Main Waterberg basin, and shows many similarities with coarse sandstones of the co-eval Mogalakwena Formation in the eastern part of the study area.

The slight trend of southwards-fining from the Melinda Fault identified in the eastern part of the study area does not seem to be followed in the west. At 23°10.45'S; 28°39.05'E

(5km north-west of Glen Alpine dam), about 1.5km south of the projected line of the Melinda Fault, the Mogalakwena Formation consists of coarse sandstone and granulestone, and pebble- and cobble-sized clasts are conspicuously absent, despite the proximity of the Melinda Fault. In thin section, these westerly rocks of the Mogalakwena Formation appear to be poorly sorted with sub-angular grains of low sphericity (Figure 4.60).

Despite the fact that there appears to be a strong stratigraphic control over clast size and frequency (Figures 4.47, 4.49 and 4.51) and a weak trend of southwards-fining (Figures 4.48, 4.50 and 4.52) in the Mogalakwena conglomerate in the immediate vicinity of Blouberg Mountain in the eastern part of the study area, there appears to be less stratigraphic control and less lateral variation in coarseness of clasts in the western part of the study area.

Palaeocurrent directions for this western part of the field area, recorded from foreset directions in trough cross-bedded sandstones, are shown in Figure 4.61, and show a diagnostic unimodal direction towards the S.W., which corresponds to the palaeocurrent direction recorded in the eastern outcrops.

4.4.2: Mogalakwena strata north of the southern strand of the Melinda Fault:

The strata under investigation in this section occur north of the southern strand of the Melinda Fault under both the northern and southern foothills of Blouberg mountain. Outcrop in the southern foothills is restricted to numerous isolated outcrops underlying areas adjacent to the northern edge shear zone of the southern strand of the Melinda Fault, e.g. 23°07.30'S; 28°55.70'E on the farm Buffelshoek 261LR. Generally these strata have shallow dips (Appendix 1), in contrast to the steeply dipping and overturned Blouberg strata on the opposite side of the southern strand of the Melinda Fault.

The outcrops of Mogalakwena Formation which occur under the northern foothills of Blouberg mountain underlie the area around 23°06'S; 28°54'E on the farm Varedig

265LR, and also occur at isolated exposures at Sesuane Hill (23°04.40'S; 28°54.10'E), Mositone (23°03.02'S; 28°56.38'E) and Semaoko (23°02.70'S; 28°51.70'E). At these localities, a maximum of about 250m of sub-horizontal strata nonconformably overlie the basement and locally unconformably overlie the Blouberg Formation (Chapter 7) and are, in turn, locally unconformably overlain by the Wyllies Poort Formation of the Soutpansberg Group (Appendix 1) (Chapter 7).

The sedimentary rocks in all these locations, (underlying both the northern and southern foothills of Blouberg Mountain) are identical, and consist of sheet-like architectural elements (CHS) (Figure 4.62). Within these elements are facies of massive cobble conglomerate, locally trough cross-bedded pebble conglomerate, and trough cross-bedded coarse sandstone and granulestone.

Conglomeratic facies are only locally developed at the base of the sedimentary successions, and vary in thickness, reaching a maximum of about 10m, though they are more commonly 50cm–2m thick (Figure 4.63). Areas where the basal conglomerate is most thickly developed seem to occupy areas of low palaeotopography developed on the basement, such as at 23°05.57'S; 28°53.42'E, where clasts of up to 20cm seem to occupy a narrow (c.50m wide) N-S trending palaeovalley cut into the basement gneiss. Correspondingly, areas where basal conglomerates are thin, or even absent, seem to outcrop above localised palaeohighs in the basement. At 23°05.76'S; 28°53.47'E, a palaeotopography can clearly be seen developed on the angular unconformity between the sub-horizontal Mogalakwena Formation and the underlying, overturned Blouberg Formation. Here a post-Blouberg, pre-Mogalakwena fault (fault plane has a dip-direction of 57°→260°) with a displacement of 2m (probably with a reverse sense of movement, although there is evidence for some post-Mogalakwena normal reactivation too) appears to have created a small cliff in the palaeotopography, under which basal conglomerates of the Mogalakwena Formation have preferentially collected. Clasts within the basal conglomerate are generally vein quartz, quartzite, fuchsitic quartz, and B.I.F. (Figure 4.64), in common with Mogalakwena conglomerate developed to the south of the southern strand of the Melinda Fault.

The basal conglomerates, where developed, are interbedded with, and rapidly grade vertically into a thick (c.200m) succession of coarse- and very coarse-grained sandstone and granulestone, with well-developed trough cross-bedding (Figure 4.65). Sets are generally about 10cm thick, and commonly have heavy mineral concentrations on foresets and bedding planes (Figures 4.66 and 4.67).

Thin section data from these two areas show the similarity between the strata of these two areas. Point counting of 300 points from a thin section taken from the northern foothills of Blouberg (Fig 4.68) show that the rock is comprised of 35% quartz, 30% matrix (=clay), 21% lithic fragments (=quartzite) and 14% opaques. Point counting of 300 points from a thin section collected from Mogalakwena strata north of the southern strand of the Melinda fault in the southern foothills of Blouberg mountain (Figure 4.69) show that these rocks are composed of 50% quartz, 18% matrix (=clay), 24% lithic fragments (=quartzite) and 7% opaques. In both cases, the relatively high percentages of opaques are due to heavy mineral concentration on foresets.

Palaeocurrent analysis of the Mogalakwena strata north of the southern strand of the Melinda Fault, shown in a rose diagram in Figure 4.70, shows a unimodal current direction towards the S.W. This is parallel with palaeocurrent directions recorded in Mogalakwena sedimentary rocks to the south.

In terms of lithofacies, architectural elements and palaeocurrent directions, the sedimentary rocks discussed here are very similar to the more distal Mogalakwena lithologies in the western part of the main area of this formation in the study region (e.g. compare Figures 4.58 and 4.66). However these strata are reasonably dissimilar to the more conglomeratic Mogalakwena Formation sedimentary rocks underlying the immediately adjacent area south of the southern strand of the Melinda Fault (though palaeocurrent directions are parallel). Such dissimilarity of adjacent sedimentary rocks may account for varying opinions proposed by workers regarding the correlation of these lithologies. For example Meinster (1977) suggested that these northerly sedimentary

rocks predate the Blouberg (*sensu strictu*) lithologies to the south (Section 1.3.2), and Callaghan and Brandl (1991) suggested that these rocks correlate with the Soutpansberg Group (i.e. post-dating the Blouberg Formation) (Section 1.3.3). Significantly, Jansen (1976) also correlated the strata discussed here (his 'Varedig Formation') with the Mogalakwena Formation (Section 1.3.1).

It is considered unlikely that these strata to the north of the southern strand of the Melinda Fault can be correlated with any of the siliciclastic strata of the lower Soutpansberg Group (e.g. the Fundudzi Formation; Table 1.3) as proposed by Brandl (1991). There is generally a close match in lithofacies, architectural elements and palaeocurrent directions between the distal lithofacies of the Mogalakwena Formation and the strata described here. In contrast, the Fundudzi Formation is generally quartzitic, or composed of fine- to medium-grained sandstone and are pale in colour, and is only rarely conglomeratic (Brandl, 1987).

Figure 4.1: Trough cross-bedded coarse sandstone and granulestone in the Setlaole Formation at 23°09.67'S; 29°03.50'E. Hammer is 30cm long.

Figure 4.2: Detail of foliated clasts in Setlaole Formation at 23°09.67'S; 29°03.50'E. Note the general poorly-sorted, immature nature of the lithology. Pen is 15cm long.

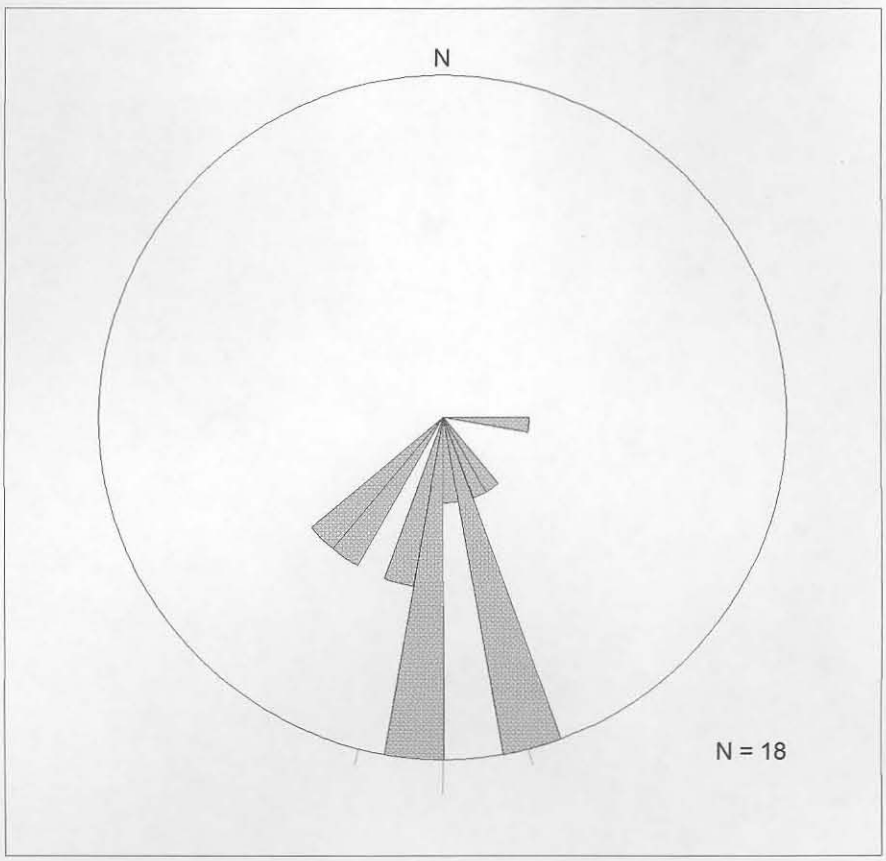

Figure 4.3: Rose diagram to show palaeocurrent directions recorded in the Setlaole Formation (in areas other than the type locality: see text). Principal direction (vector mean) is shown.

Figure 4.4: The lower nonconformity between the Setlaole Formation and the underlying basement. The basement consists of pink granitic material, with darker amphibolitic rocks locally juxtaposed by pre-Setlaole faulting. The Setlaole Formation is marked by a basal pebble conglomerate with quartz and granitic pebbles developed in hollows on the palaeosurface, and rapidly grades up into mudrock (dark upper layer). Recorded at 23°20.36'S; 28°58.00'E. Hammer is 30cm long.

Figure 4.5: Trough cross-bedded sets in coarse- to very coarse-grained sandstone of the Setlaole Formation at 23°20.36'S; 28°58.00'E. Lens cap is 5cm wide.

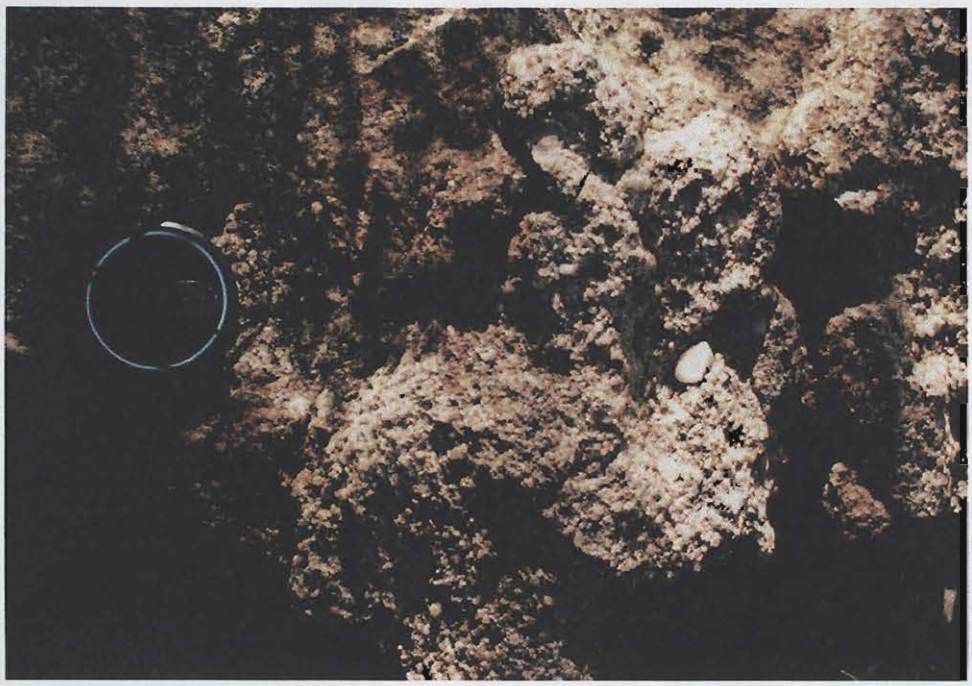

Figure 4.6: Pale-coloured pebbly granulestone facies in the Setlaole Formation at 23°20.90'S; 28°58.50'E. Lens cap is 5cm wide.

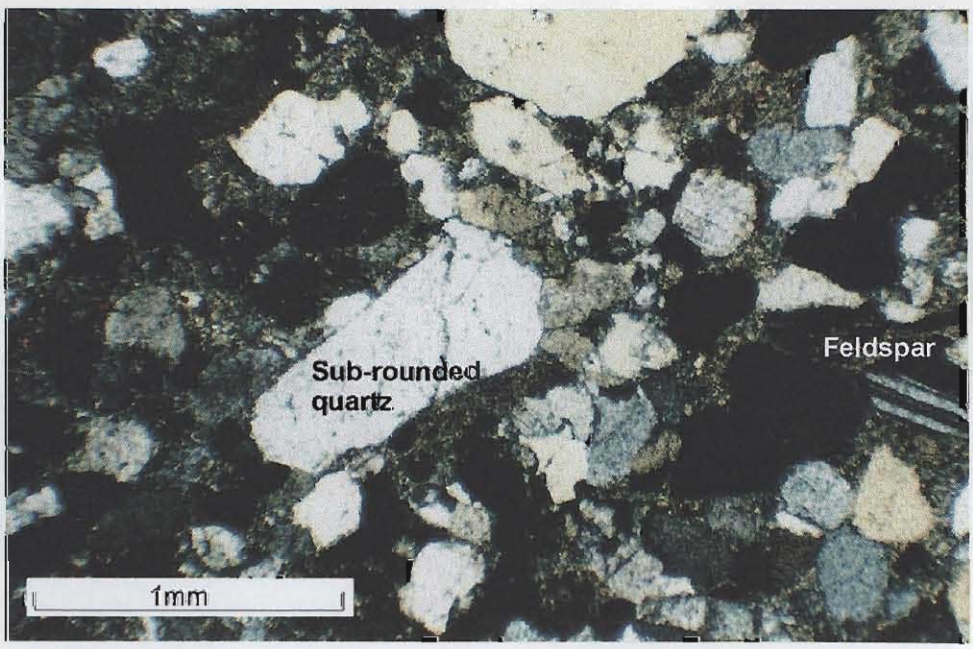

Figure 4.8: Photomicrograph from the Setlaole Formation, showing poor sorting and sub-angular to sub-rounded quartz grains and rare feldspar grains. Sample taken from 23°16.33'S; 28°59.94'E.

Figure 4.7: Rose diagram showing the palaeocurrent directions recorded from trough cross-beds in the Setlaole Formation at the type locality (23°20.90'S; 28°48.50'E). Principal direction (vector mean) is shown.

Figure 4.9: Strata which outcrops at 23°06.54'S; 28°49.38'E, comprised of pale-coloured pebbly granulestone. c.f. Figure 4.6. Lens cap is 5cm wide.

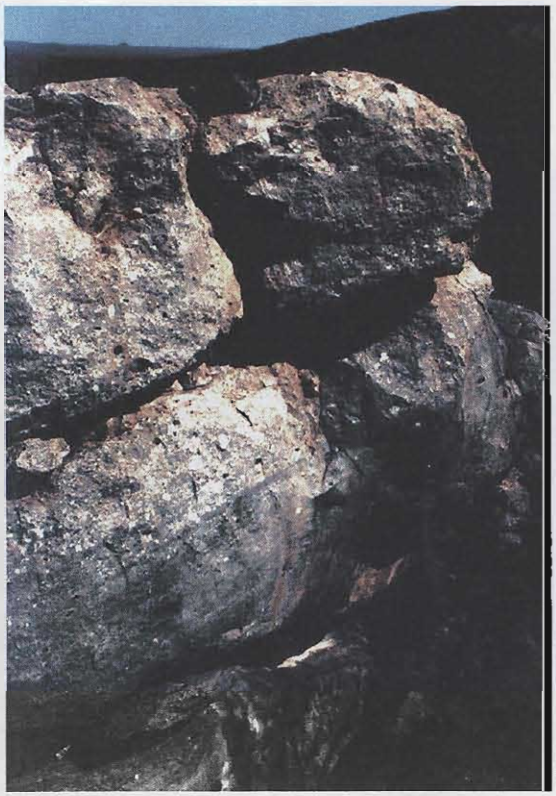

Figure 4.10: Pale coloured trough cross-bedded conglomerate and granulestone are interbedded with darker (purplish) horizontally laminated sandstone. Recorded at 23°06.54'S; 28°49.38'E. Rucksack at top of cliff for scale.

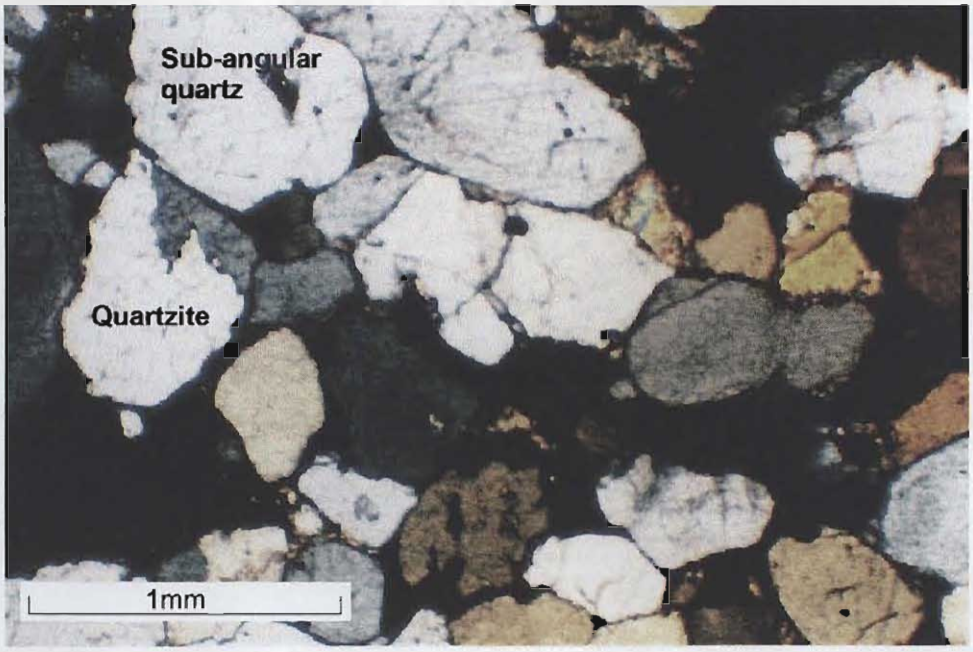

Figure 4.11: Photomicrograph from a sandstone clast from a conglomerate layer within the Setlaole Formation. Pebble is composed of sub-angular quartz grains, quartzitic lithic fragments and opaque minerals.

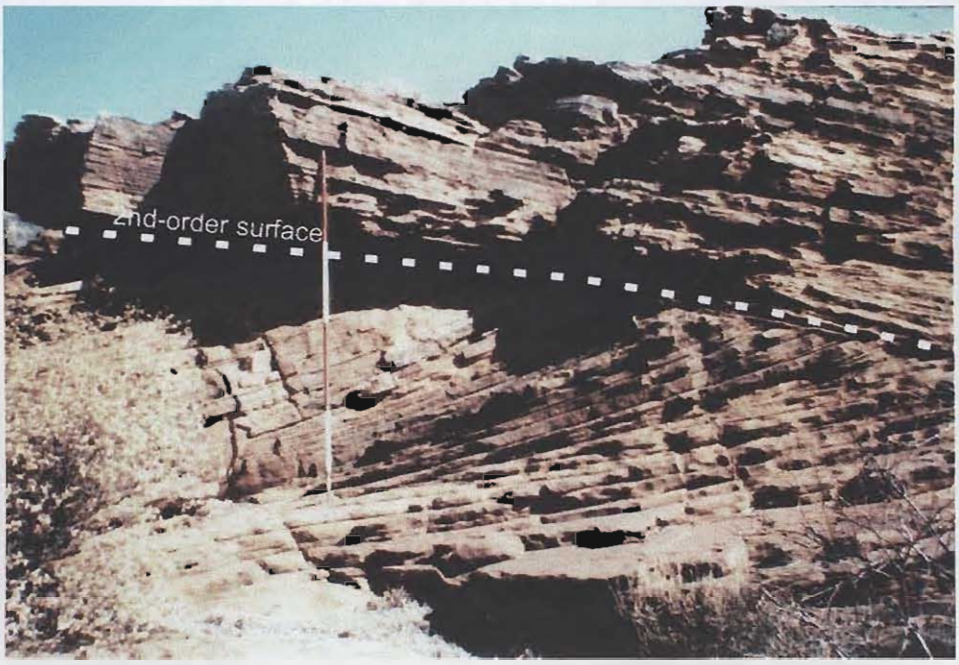

Figure 4.13: Second-order surface developed between two sets of large-scale trough cross-beds in the Makgabeng Formation. Recorded at 23°15.34'S; 28°48.70'E. Ranging pole is 2m long.

Depth		Lithology	Colour	Bed Thickness	Sorting	Comments
0						Mogolakwena Formation,
20		Cong			Poor	Makgabeng Formation at 29m
		M.sst.	Greyish red		Good	SSD: 29-31.5m, Mas:31.5-33m
		M.sst.			Good	Reduction marks up to 628m
40		M.sst.			Good	is frequent
		F.sst.	Pale Red	2mm	Good	Mas: 45-45.4m. SSD:49-50.48m
		F.sst.			Good	
60		F.sst.			Good	
		F.sst.			Good	
		F.sst.		2-20mm	Good	
80		F.sst.			Good	
		F.sst.		1-10mm	Good	
		F.sst.			Good	Interdune material + clay at 90m
100		F.sst.			Good	Interdune material + clay at 106m
		M.sst.	Moderate	2-10mm	Good	Mas: 107.7-111.2m; 112-114m
		M.sst.	red		Good	
120		M.sst.	Dusky Red		Good	Mas:120-122m
		M.sst.			Good	
		M.sst.			Good	
140		F.sst.			Good	
		F.sst.	Moderate		Good	
		F.sst.	red		Good	
160		F.sst.		2-5mm	Good	Mas: 164.7-165m; 170-175m
		F.sst.	Grey Red		Good	(massive with oblong,angular
		F.sst.			Good	clasts of silt/mud/sandstone)
180		F.sst.			Good	Mas:187.6-189m, 193-194m
		F.sst.		3mm	Good	
		F.sst.	Pinkish		Good	
200		F.sst.	grey		Good	Mas: 210-210.5m
		F.sst.		2-3mm	Good	
		F.sst.	Pale Red		Good	
220		F.sst.			Good	Mas: 236-240m
		F.sst.	Grey Red		Good	
		F.sst.		2-10mm	Good	
240		M.sst.			Good	Mas: 246-253m
		M.sst.	Dusky Red		Good	
		M.sst.			Good	
260		M.sst.	Grey red		Good	Mas: 266-266.2m, 267-276.4m;
		F.sst.		5mm	Good	268.4-269m; 272-272.4;
		F.sst.		2-5mm	Good	274-274.5m; 276.5-277.5m
280		F.sst.	Light Grey		Good	Mas: 282-282.4; 285-285.7m;
		M.sst		2-10mm	Good	288-288.7m
		M.sst			Good	
300		M.sst	Grey Red		Good	Mas: 306-306.6m;
		F.sst.		2-10mm	Good	
		F.sst.	Pale Red	5mm	Mod	

320	F.sst.	Dusky red		Mod	Mas: 327-327.7; 329-330.5
	M.sst.		2mm	Mod	
	M.sst.	Pinkish		Good	SSD at 338.8-339
340	M.sst.	grey		Good	Mas: 344-346.25m; 354-355.5m;
	C.sst.	Pale Red		Good	357-357.7; 358.3-358.9m
	C.sst.		2-5mm	Good	SSD at 346.25m
360	M.sst.			Good	360-360.4m -clay rich
	F.sst.			Good	361.3-361.7m-conglomerate in clay
	F.sst.			Good	Mas:374.5-382.7m (SSD)
380	F.sst.			Good	Mas: 384-384.4m; 395-
	F.sst.			Mod	400m (SSD structures present).
	F.sst.		2-10mm	Mod	
400	F.sst.		5mm	Mod	
	F.sst.			Good	
	F.sst.			Good	
420	F.sst.		2-10mm	Good	426-435m= red siltstone, with
	Silt			Good	interlayered sandstone
	M.sst.			Good	SSD at 433m
440	M.sst.			Good	
	M.sst.		1-3mm	Good	
	Diabase	Grey			
460	Diabase			Good	
	Diabase			Good	
	Diabase			Good	
480	Diabase			Good	
	Diabase			Good	
	F.sst.	Light	2mm	Mod	Altered Sandstone
500	F.sst.	brownish		Mod	
	F.sst.	grey	2-10mm	Mod	
	F.sst.			Mod	Mas: 517-519m
520	F.sst.			Mod	
	F.sst.	Grey red		Mod	
	M.sst.	Dusky red		Mod	
540	F.sst.			Good	Mas: 541.2-542.2m; 548-548.3m
	F.sst.	Greyish orange	1mm	Good	554.2 -554.8m; 556-556.4m
	F.sst.	Dusky red		Good	Interdune clay at 551m and 557m
560	F.sst.	Greyish orange		Good	Mas: 563-563.4m
	F.sst.	Pale Red	2-5mm	Good	
	F.sst.	Greyish orange	2-20mm	Good	
580	Silt	Moderate Red		Good	
	Shale		2-10mm	Good	
	Shale			Good	
600	F.sst.			Good	
	F.sst.	Pinkish grey		Good	
	F.sst.	Greyish Orange		Good	
620	F.sst.			Good	
	F.sst.			Mod	
	F.sst.		1-20mm	Mod	Mas: 638-638.3
640	M.sst.			Mod	Setlaole Formation, at 639m
	M.sst.		2mm	Mod	Distinct colour change from 'red'
	M.sst.	Pale red		Mod	to 'white' at 639m
660	F.sst.			Mod	

		F.sst.			Mod
		M.sst.	Pale brown		Mod
680		F.sst.			Mod
		F.sst.	Medium grey	2-10mm	Mod
		M.sst.	Dark yellowish		Mod
700		M.sst.	brown		Mod
		M.sst.	Medium grey		Mod
		F.sst.			Good
720		F.sst.	Pale brown		Good
		F.sst.	Dark yellowish		Good
		F.sst.	brown	2-5mm	Good
740		F.sst.	Light grey		Good
		F.sst.		2-10mm	Mod
		F.sst.	Pale brown		Mod
760		F.sst.			Mod
		M.sst.	Reddish brown		Mod
		Diabase	Grey		
780		F.sst.	Pale brown	2-4mm	Mod
		F.sst.			Mod
		Diabase	Grey		
800		F.sst.	Light grey	2-10mm	Mod
		F.sst.	Light brown		Mod
		Diabase	Grey		
820		F.sst.	Medium brown	2-10mm	Mod
		F.sst.			Mod
		F.sst.	Light brown	5-10mm	Mod
840		F.sst.			Mod
		Diabase	Grey		
		Diabase			
860		Diabase			
		Diabase			
		Diabase			
880		Diabase			
		Diabase			
		Diabase			
900		Diabase			
		Diabase			
		Diabase			
920		Diabase			
		Diabase			
		Diabase			
940		Diabase			
		Diabase			
		Diabase			
960		Diabase			
		Diabase			
		Diabase			
980		Diabase			
		Diabase			
		Diabase			
1000		Diabase			
		Diabase			

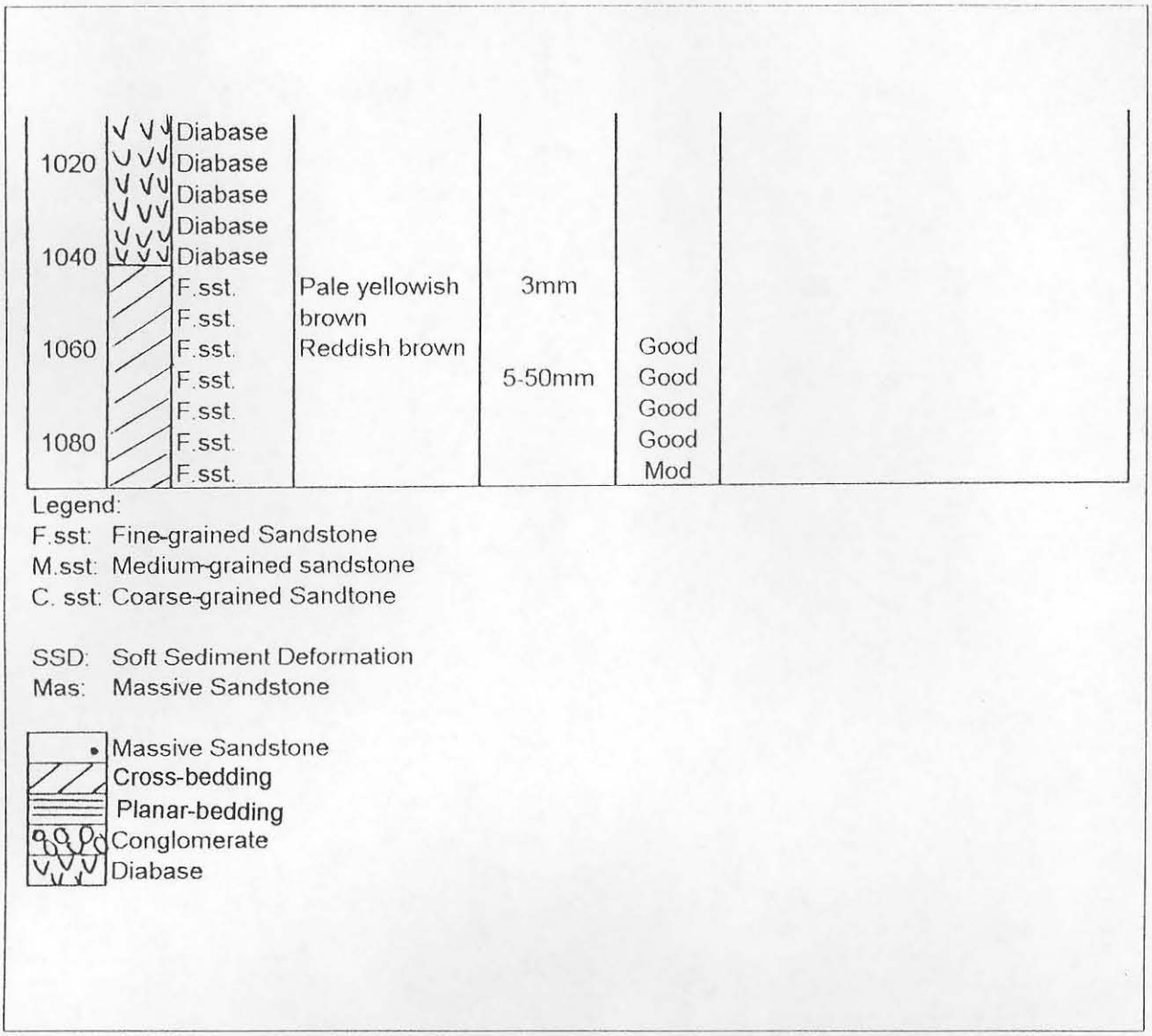

Figure 4.12: Borehole log from drill core through the Makgabeng Formation from farm Vleypan 411 (23° 28'S; 28° 37'E).

a.

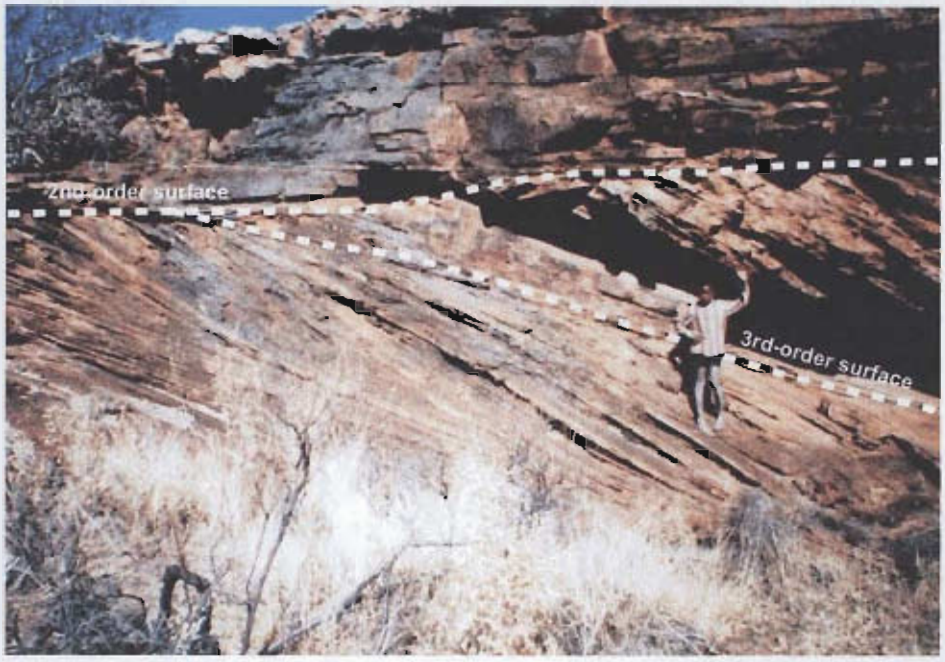

b.

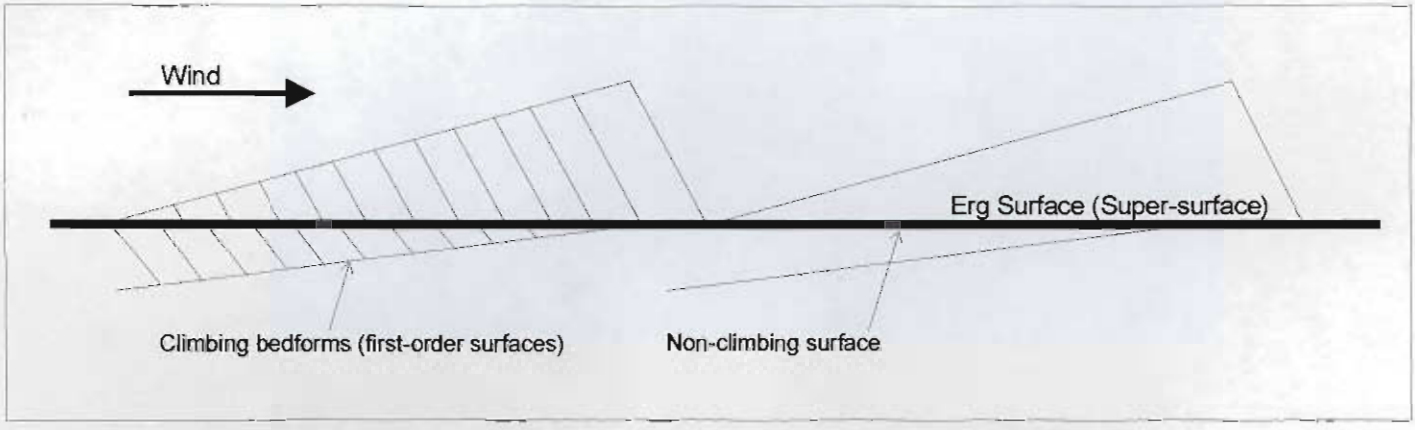

Figure 4.14a: Third-order (reactivation) surfaces developed within sets of large-scale trough cross-bedded sandstones in the Makgabeng Formation. Note the second-order surface which crosscuts them.

Figure 4.14b: Sketch illustrating climbing bedforms and horizontal nature of super-surfaces (e.g. erg surface) (after Brookfield, 1977).

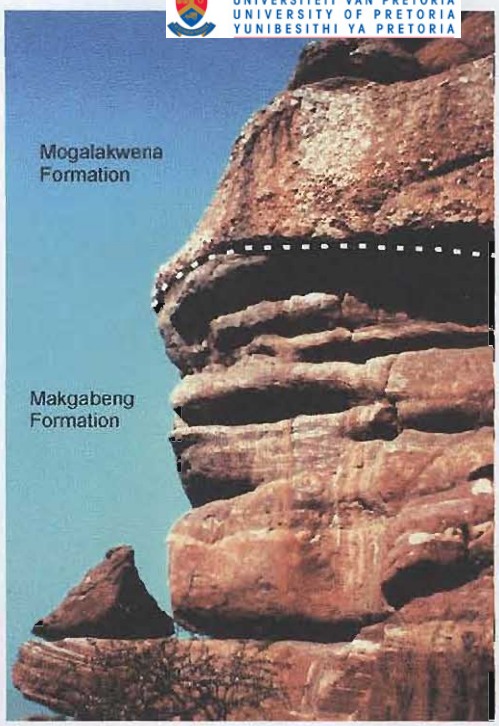

Figure 4.15: Super-surface developed between the Makgabeng Formation (bottom) and the Mogalakwena Formation (conglomeratic) at 23°11.47'S; 28°52.38'E. Cliff section is about 5m high.

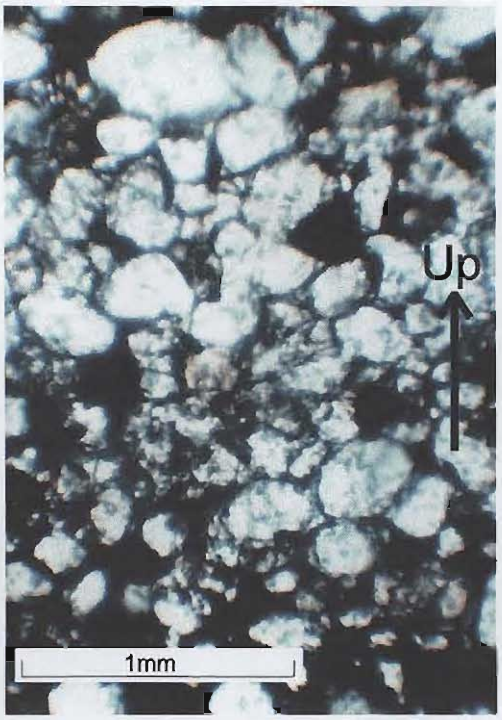

Figure 4.16: Photomicrograph from the large-scale cross-bedded sandstone facies association in the Makgabeng Formation, showing inverse-grading of sand grains within laminations. Quartz grains are generally well-sorted, rounded and have high sphericity.

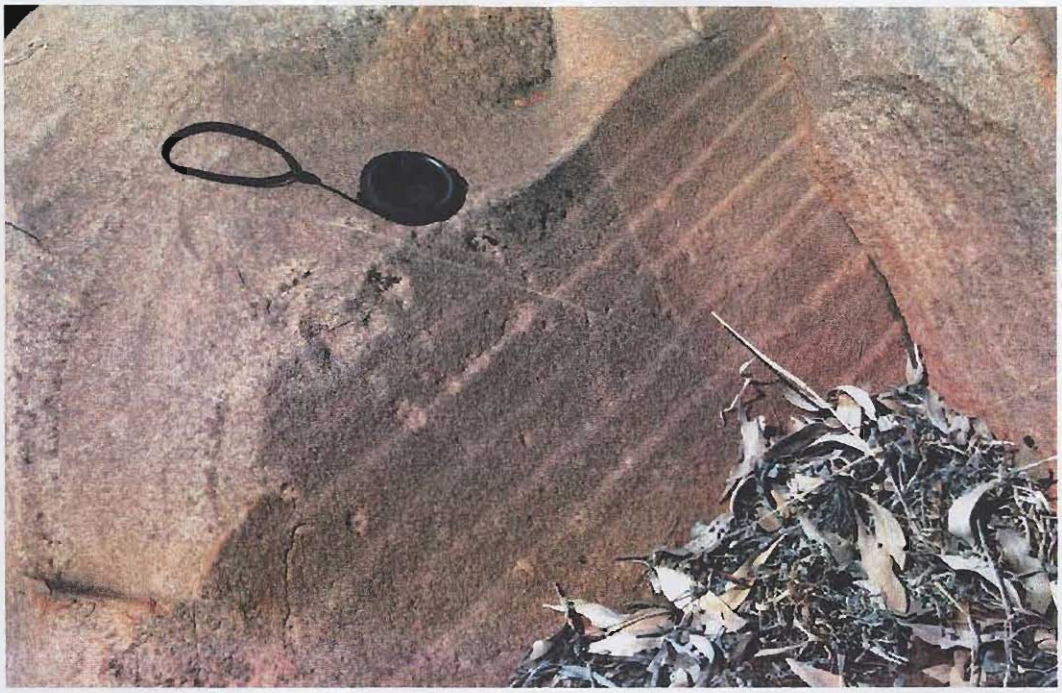

Figure 4.17: Asymmetric ripple marks in the Makgabeng Formation. Lens cap is 5cm wide.

Figure 4.18: Steeply-inclined (<30°) cross-beds comprising inversely-graded foresets in the Makgabeng Formation. View is perpendicular to the dip direction.

Figure 4.19: Wedge-shaped strata (pale-coloured rock) tapering in a down-dip direction.

Figure 4.21: Horizontally-bedded and rippled mudrocks with interbedded sandstone at 23°13.60'S; 28°52.80'E. Camera bag is 25cm high.

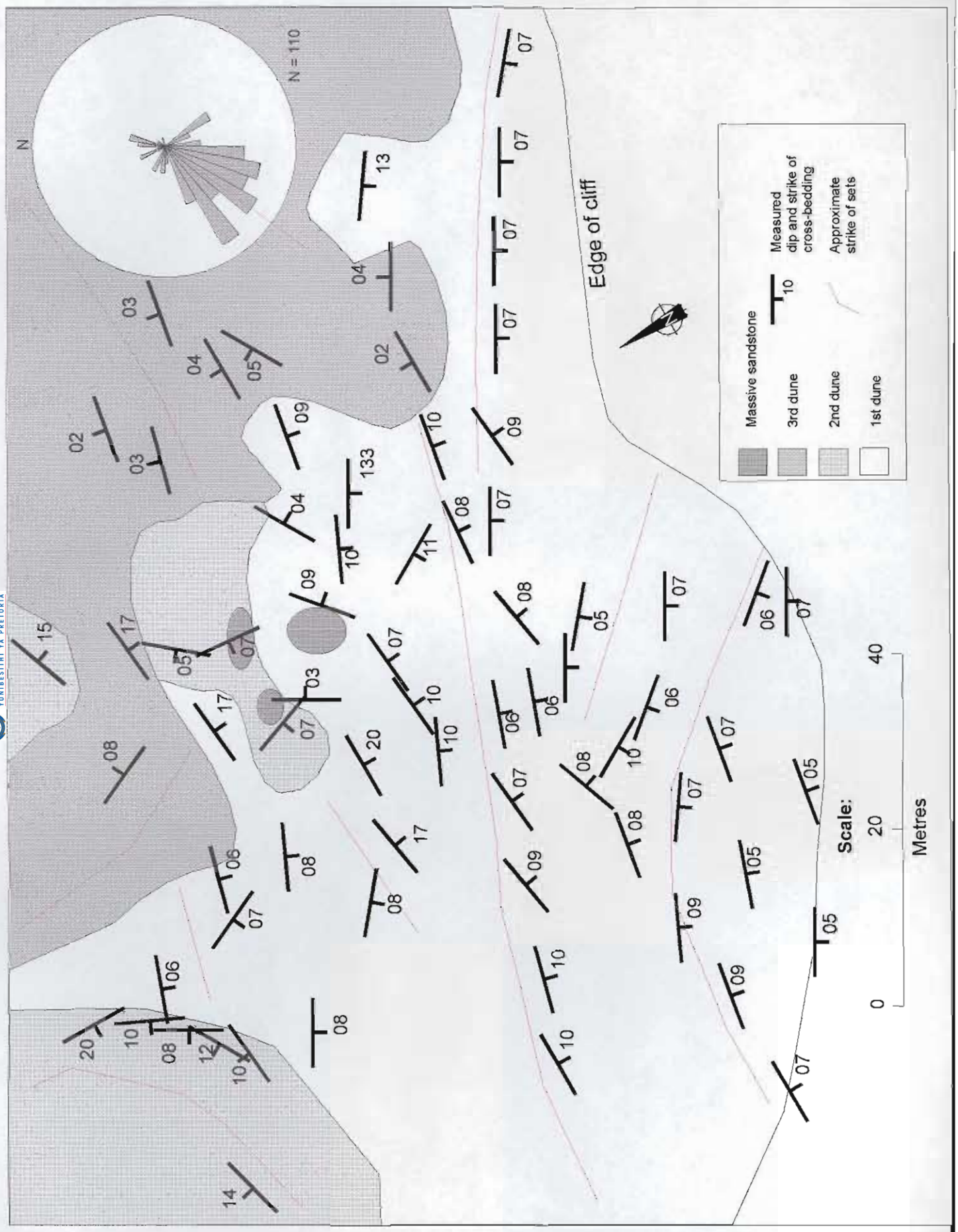

Figure 4.20: Map showing relationships between sets of large-scale trough cross-beds in the Makgabeng Formation at 23° 15.34'S; 28° 48.70'E. Rose diagram shows the orientation of foreset dip directionsfor foresets (planar and trough cross-beds) in the Makgabeng Formation. The principal direction (vector mean) is indicated.

Figure 4.22: Current ripples in mudrock in the Makgabeng Formation, with superimposed desiccation cracks. Pen is 15cm long.

Figure 4.23: Muddy roll-up structures in mudrock and sandstone in the Makgabeng Formation. Mud laminations contain of up to 720° of curvature, and "roll-ups" are orientated parallel to each other.

Figure 4.24: Muddy roll-up structures in mudrock and sandstone in the Makgabeng Formation.

Figure 4.25: Evaporite casts (possibly of gypsum crystals) developed in the rippled mudrock and sandstone facies association of the Makgabeng Formation.

Figure 4.26: Massive sandstone facies exposed in the top-most horizontal beds in this picture (about 5 beds between 30cm and 1m thick). Recorded at 23°15.34'S; 28°48.70'E.

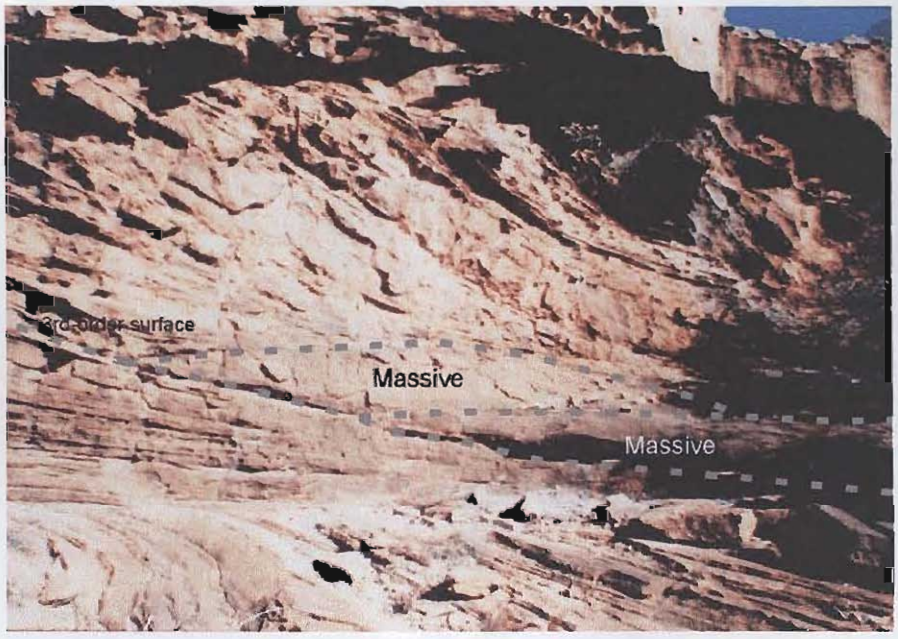

Figure 4.27: Two lens-shaped massive sandstone beds onlap to the left onto third-order surfaces. Massive beds are both about 40cm thick at their thickest point.

Figure 4.28: Channelised massive sandstone associated with more steeply-dipping inversely graded strata. View is in the down-dip direction.

Figure 4.29: The erosive nature of the massive sandstone is illustrated by the fact that the upper massive sandstone has cut down through the low-angled toeset cross-strata into more steeply-dipping cross-bedding of an older set. Pen is 15cm long.

Figure 4.30: Soft sediment deformation in the Makgabeng Formation. Laminations appear to have slumped, verging in a direction parallel to the dip-direction of the foreset. The preservation of laminae in the slumped strata suggests that they were cohesive, possibly due to the presence of water.

Figure 4.31: Channelised contact between inversely graded strata (bottom) and more massive strata of the pebbly sandstone facies association (top). Recorded at 23°16.01'S; 28°52.30'E. Hammer is 30cm long.

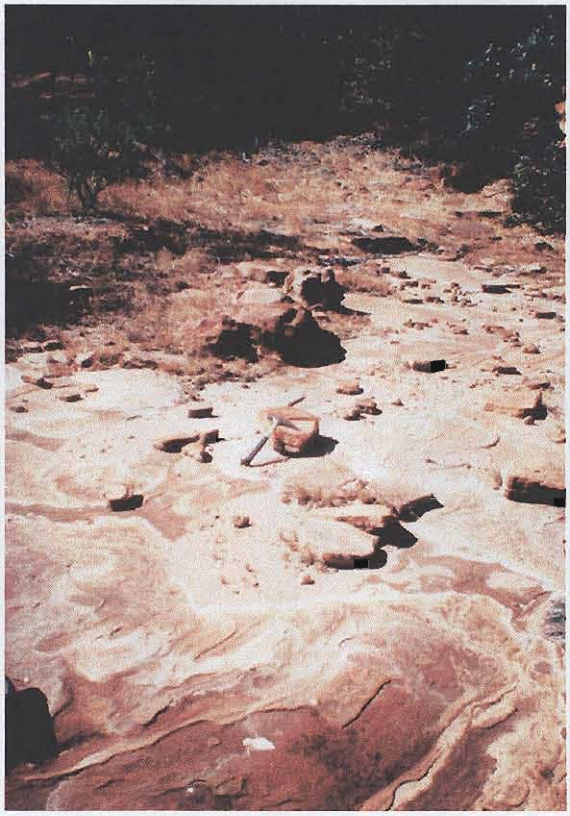

Figure 4.32: Planar laminated sandstone containing rare quartz pebbles. Recorded at 23°16.01'S; 28°52.30'E. Hammer is 30cm long.

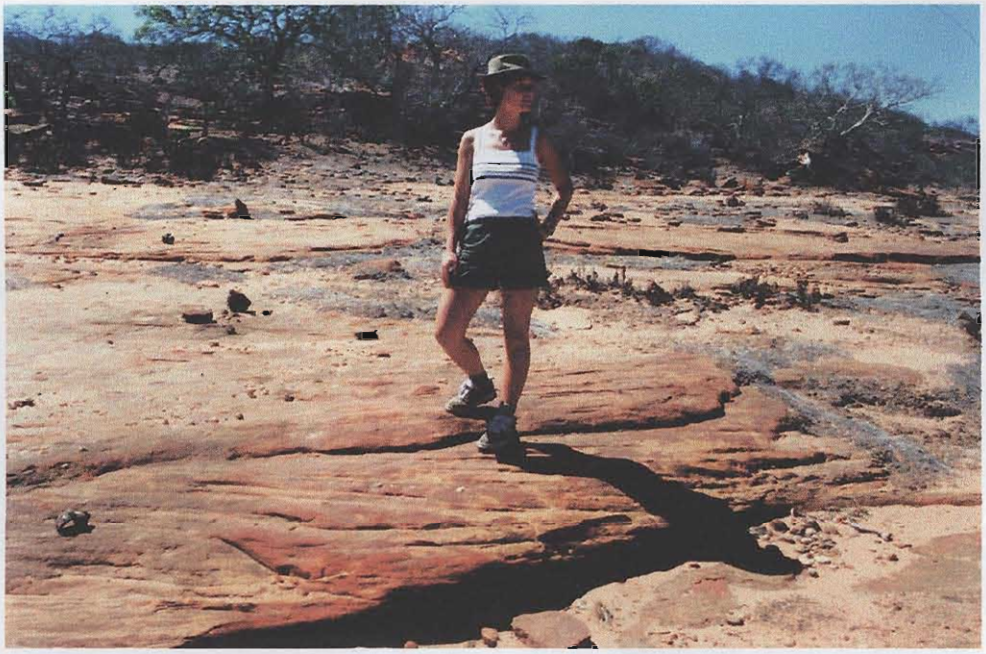

Figure 4.33: Relatively small (<50cm) set of planar cross-bedding, with quartz pebbles on foresets in the pebbly sandstone facies association. Recorded at 23°16.07'S; 28°52.42'E.

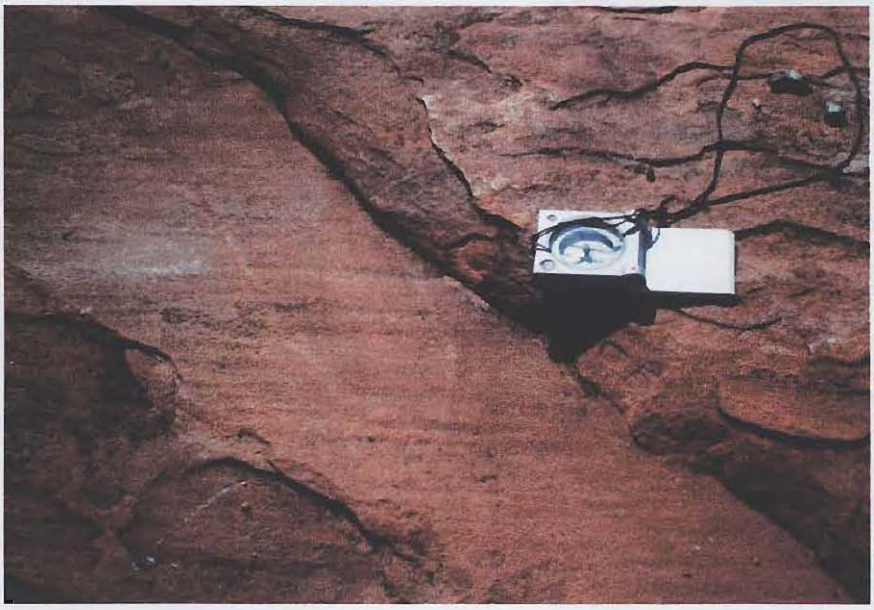

Figure 4.34: Parting lineation developed on planar-bedding surfaces in the pebbly sandstone facies association. Recorded at 23°16.07'S; 28°52.42'E. Compass is 8cm wide, and points north, indicating a north-south-trending current.

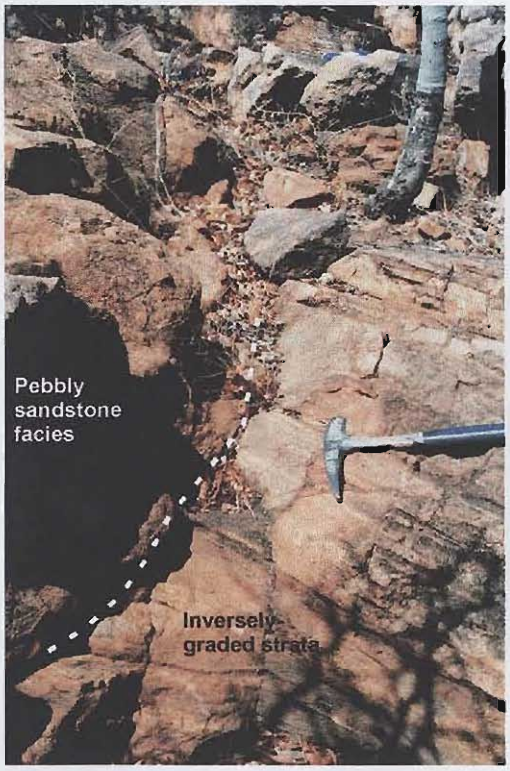

Figure 4.36: Steeply-inclined inversely-graded strata are overlain (and partly cut into by channels) by more massive sandstone of the pebbly sandstone facies association. Recorded at 23°16.01'S; 28°52.30'E. Hammer is 30cm long.

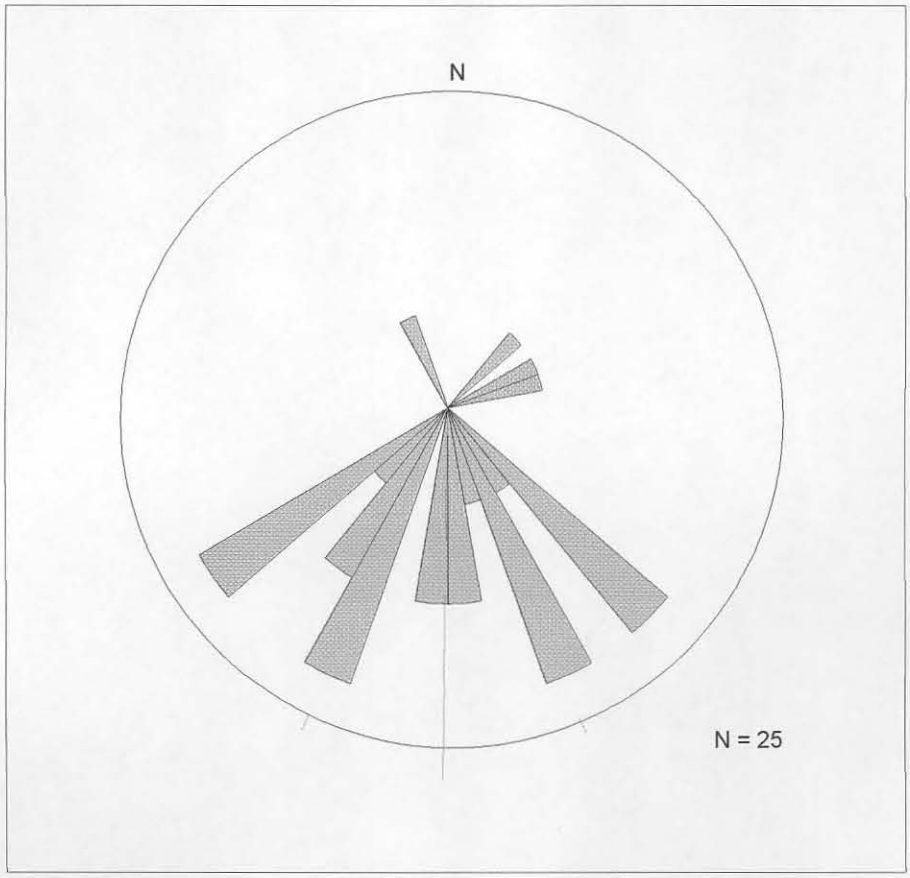

Figure 4.35: Rose diagram showing palaeocurrent directions recorded from trough cross-beds in the pebbly sandstone facies association. Principal direction (vector mean) is shown.

Figure 4.37: Interbedded conglomerate and sandstone sheet-like elements of the Mogalakwena Formation are exposed in steep-sided mesas at 23°16.25'S; 28°50.50'E. Cliffs are c.200m high.

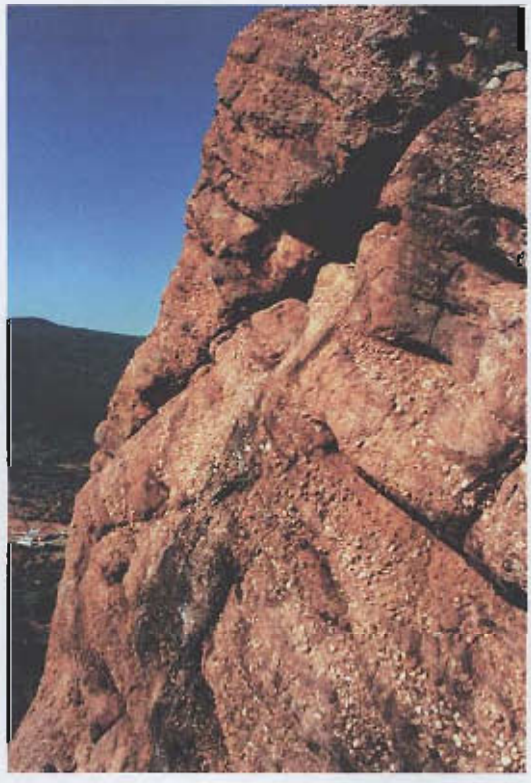

Figure 4.38: Interbedded sandstone and conglomerate sheets at 23°08.45'S; 28°54.15'E. Cliff is c. 10m high.

Figure 4.39: Large-scale conglomerate-filled channel forms (c. 5m deep, 50m wide) within sheet-like architectural elements in the Mogalakwena Formation, preserved at 23°08.21'S; 28°54.49'E.

Figure 4.40: Rare imbricated conglomerates are interbedded with cross-bedded sandstone sheets at 23°11.23'S; 28°52.44'E. Camera bag is 25cm high.

Figure 4.41: Well-rounded, massively bedded quartz and quartzite cobbles of high sphericity in conglomerate sheet of the Mogalakwena Formation at 23°11.23'S; 28°52.44'E. Note book is 20cm high.

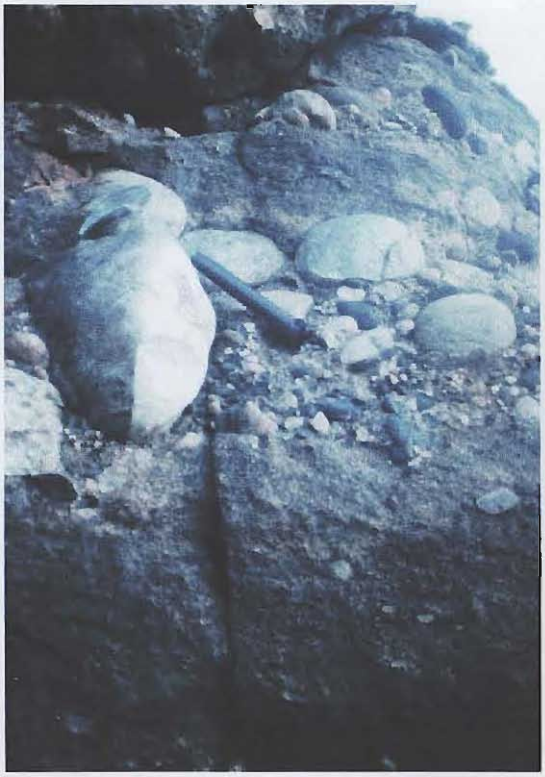

Figure 4.42: Cobbles of quartz, quartzite and B.I.F. in the Mogalakwena Formation at 23°06.69'S; 28°00.51'E.

Figure 4.43: Plan view of trough cross-bedding in sandy sheets in the Mogalakwena Formation. Recorded at 23°09.01'S; 28°42.01'E. Compass points north, indicating that palaeocurrent direction was to the S.W.

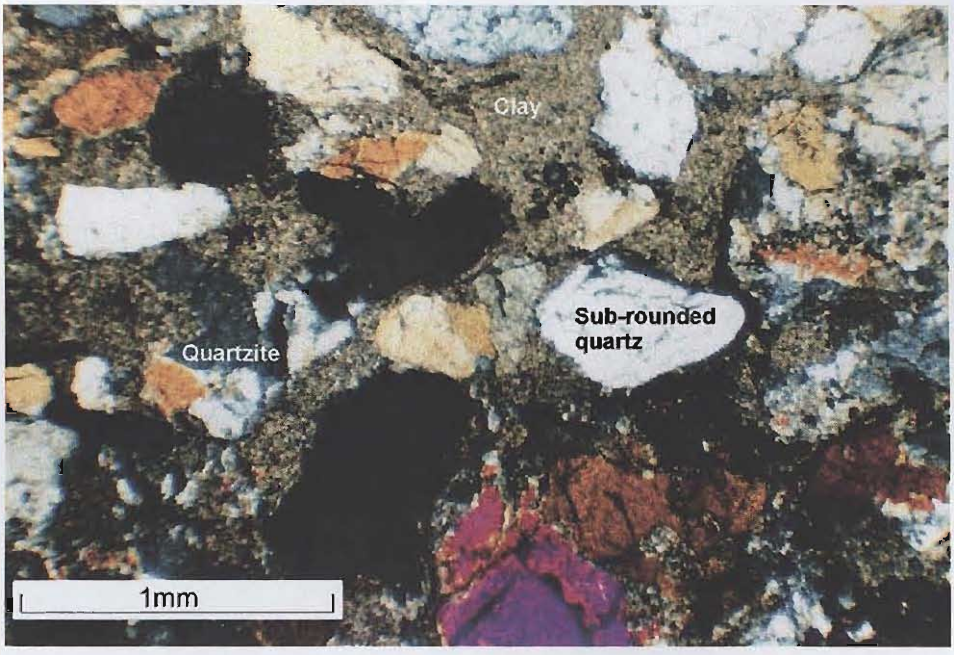

Figure 4.44: Photomicrograph of rock from sandy sheets, showing fairly well-sorted, sub-angular to sub-rounded quartz and quartzite grains (section is slightly too thick), with a high percentage of clay matrix.

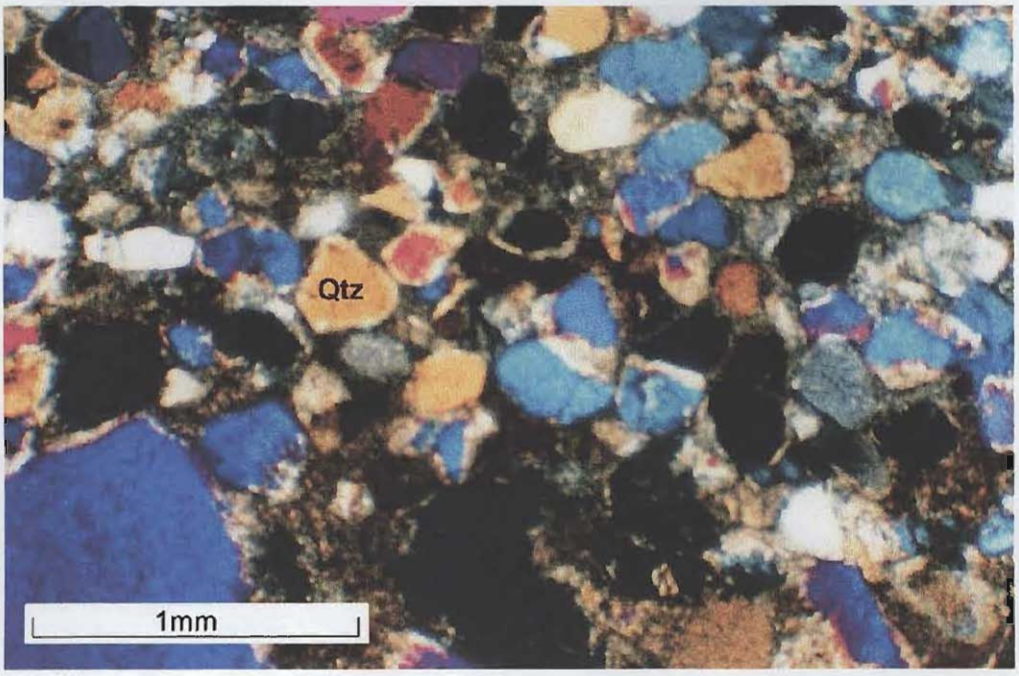

Figure 4.45: Photomicrograph of matrix from Mogalakwena granulestone, showing fairly well-sorted, sub-rounded quartz grains of medium sphericity. Section is slightly too thick.

Figure 4.46: Map showing the outcrop of the Mogalakwena Formation and the location of recording sites for pebble survey.

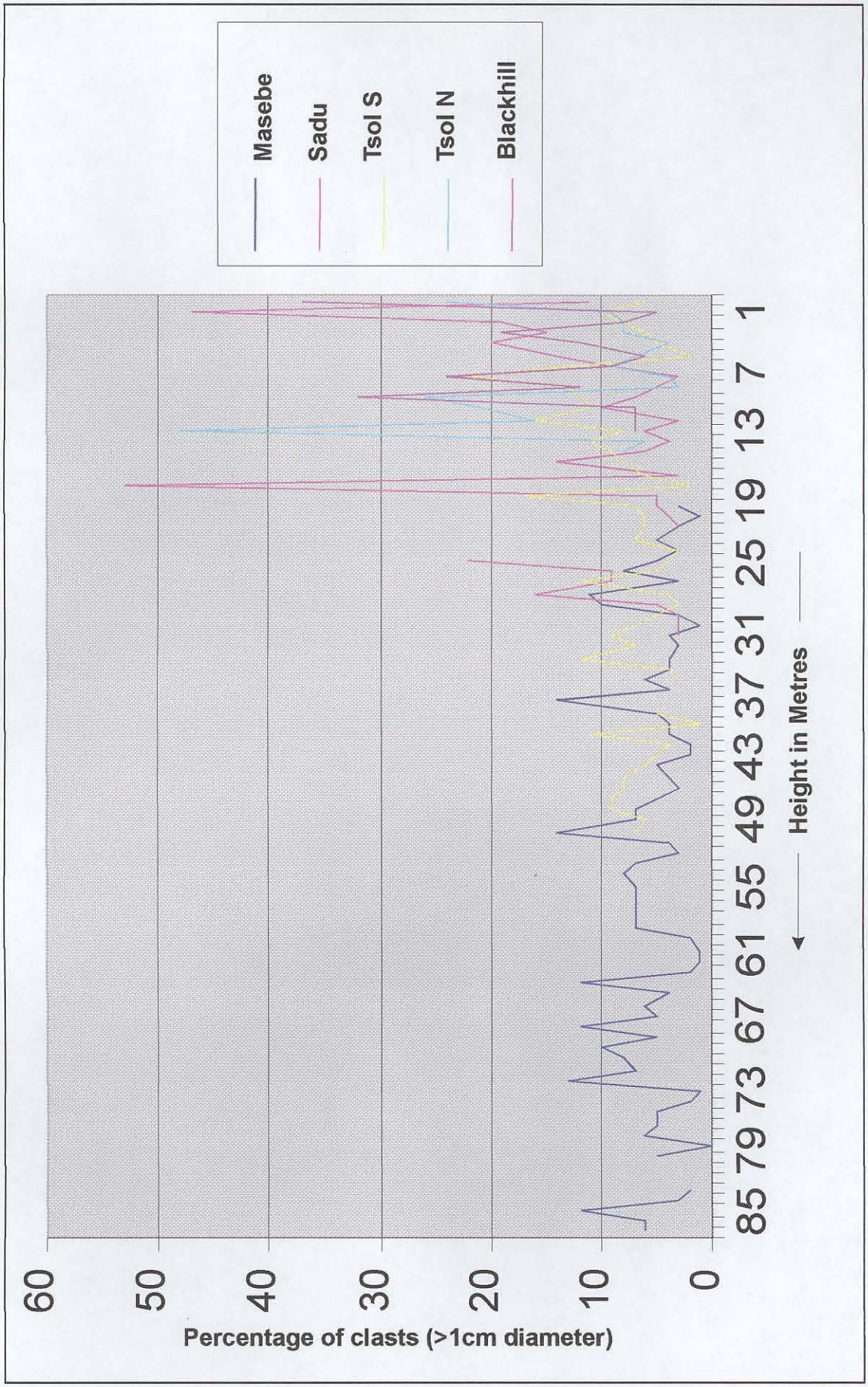

Figure 4.47: Graph to show the variance in the percentage of clasts >1cm diameter, with stratigraphic height in the Mogalakwena Formation.

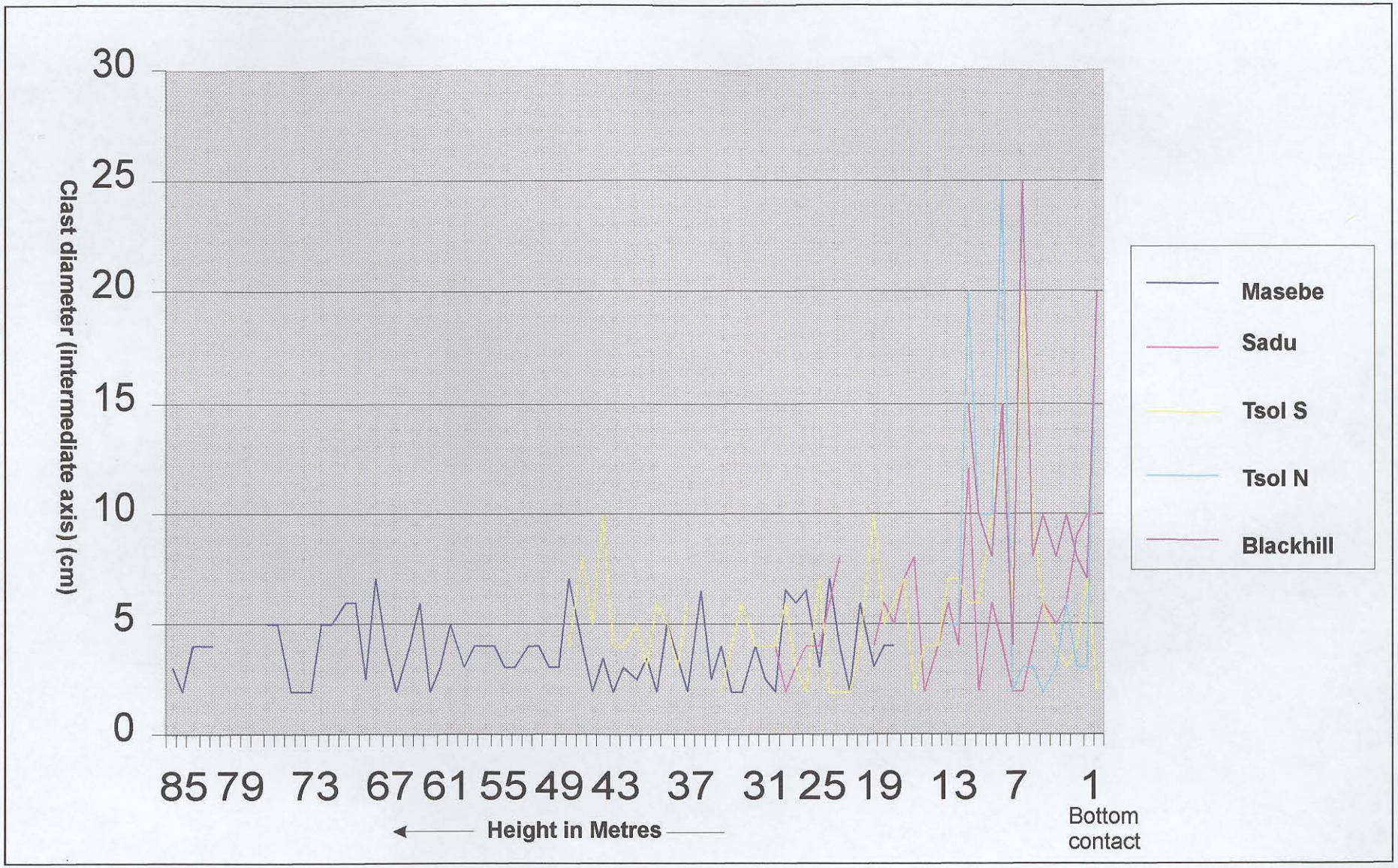

Figure 4.49: Graph to show variance in clast size (intermediate axis) with stratigraphic height in the Mogalakwena Formation.

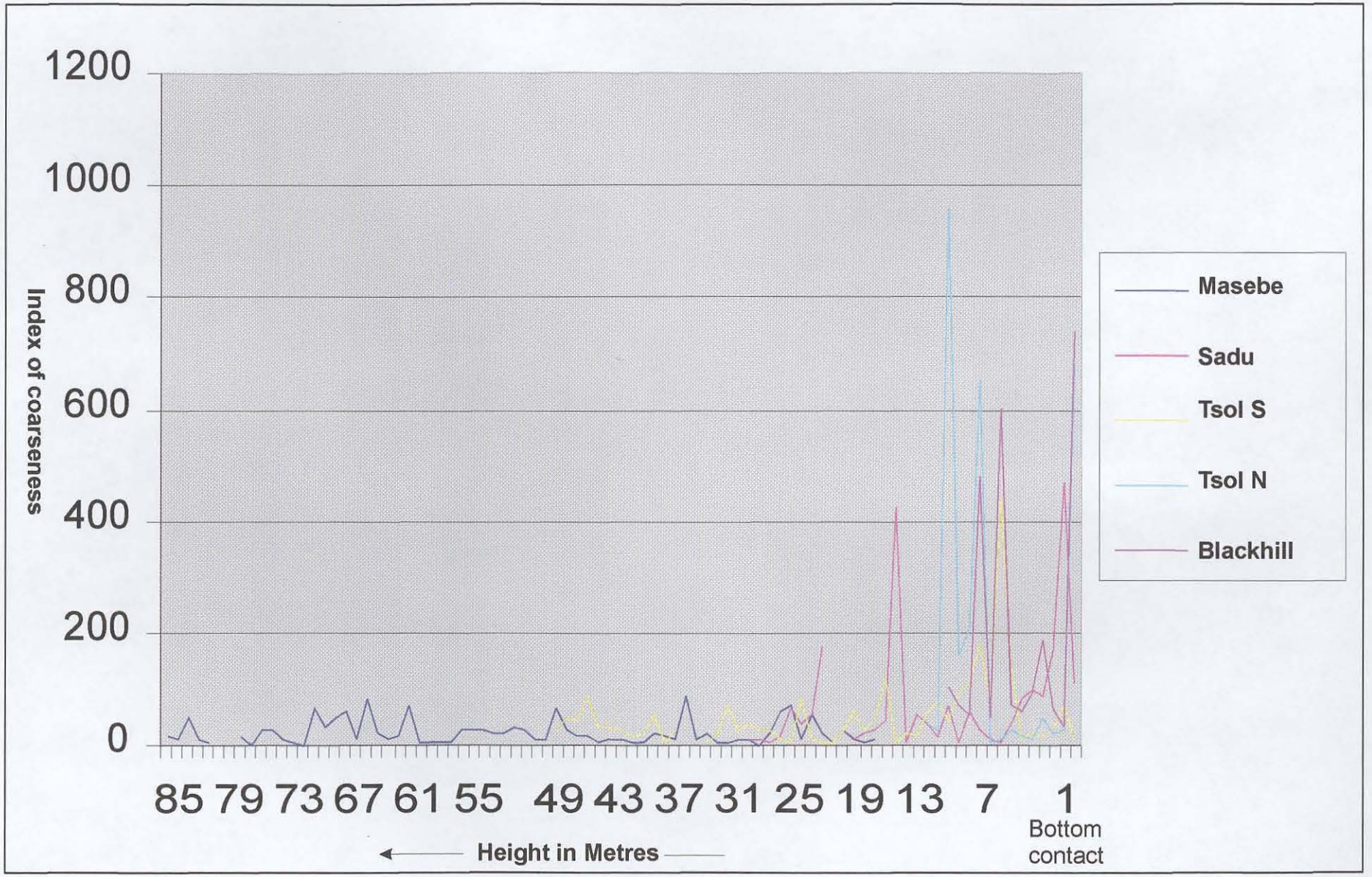

Figure 4.51: Graph to show variance of 'Index of Coarseness' (intermediate axis length x % of clasts) with stratigraphic height in the Mogalakwena Formation.

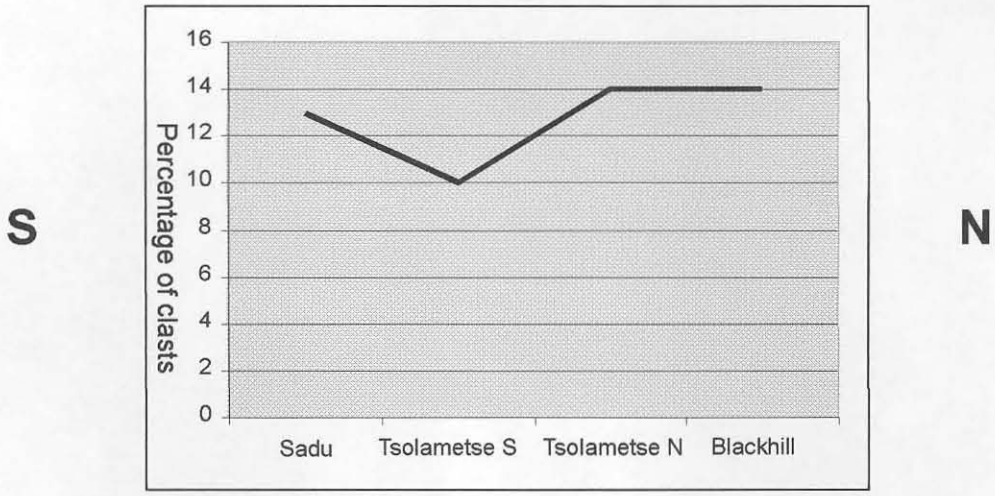

Figure 4.48: Graph showing variance in percentage of clasts from N to S.

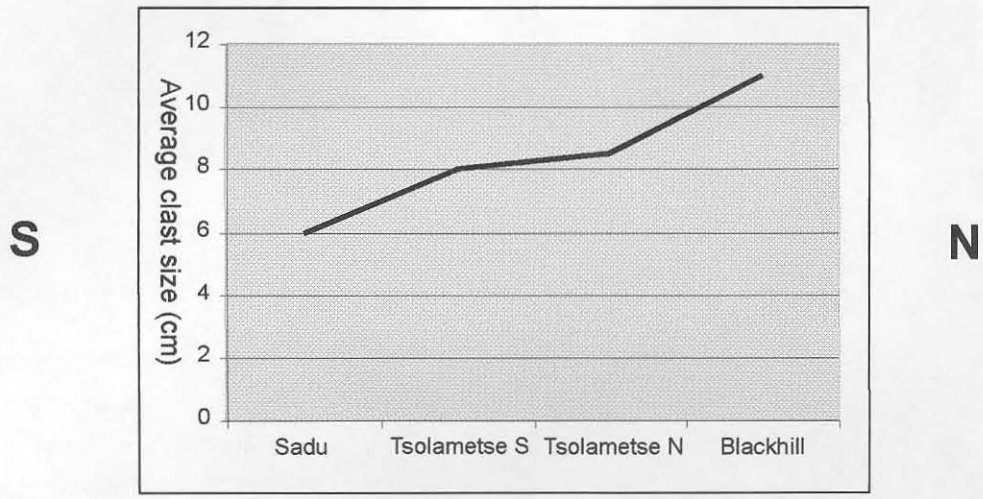

Figure 4.50: Graph showing variance in average size of clasts from N to S.

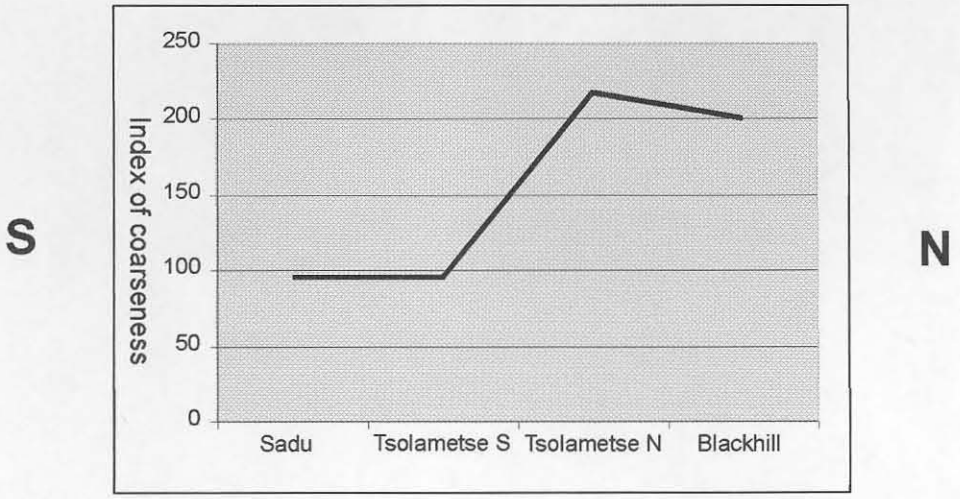

Figure 4.52: Graph to show the variance in the index of coarseness from N to S.

Figure 4.53: Graph to show variance in total percentages for each clast composition with stratigraphic height.

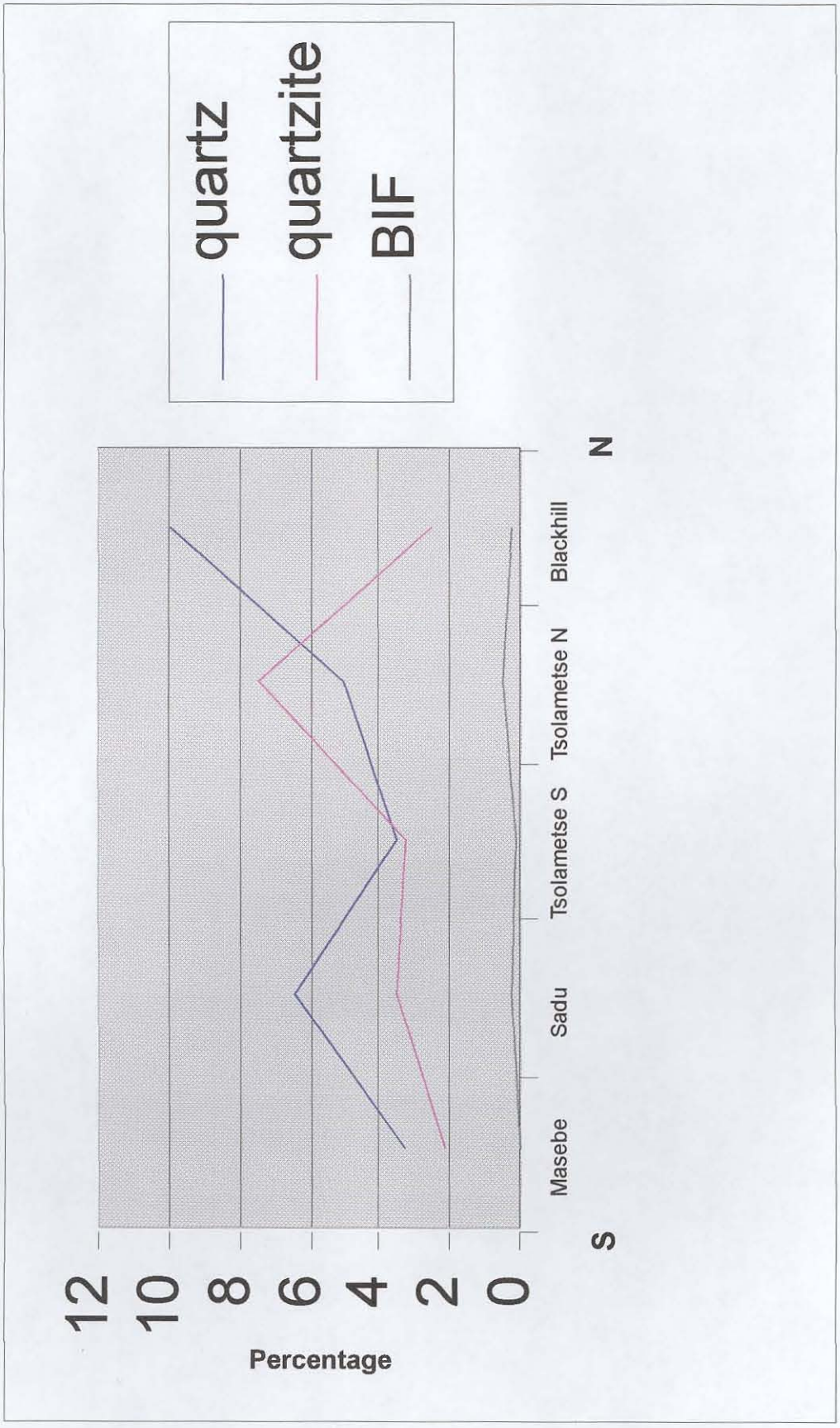

Figure 4.54: Graph to show N-S variance in quartz, quartzite and B.I.F. cobbles present in the Mogalakwena Formation.

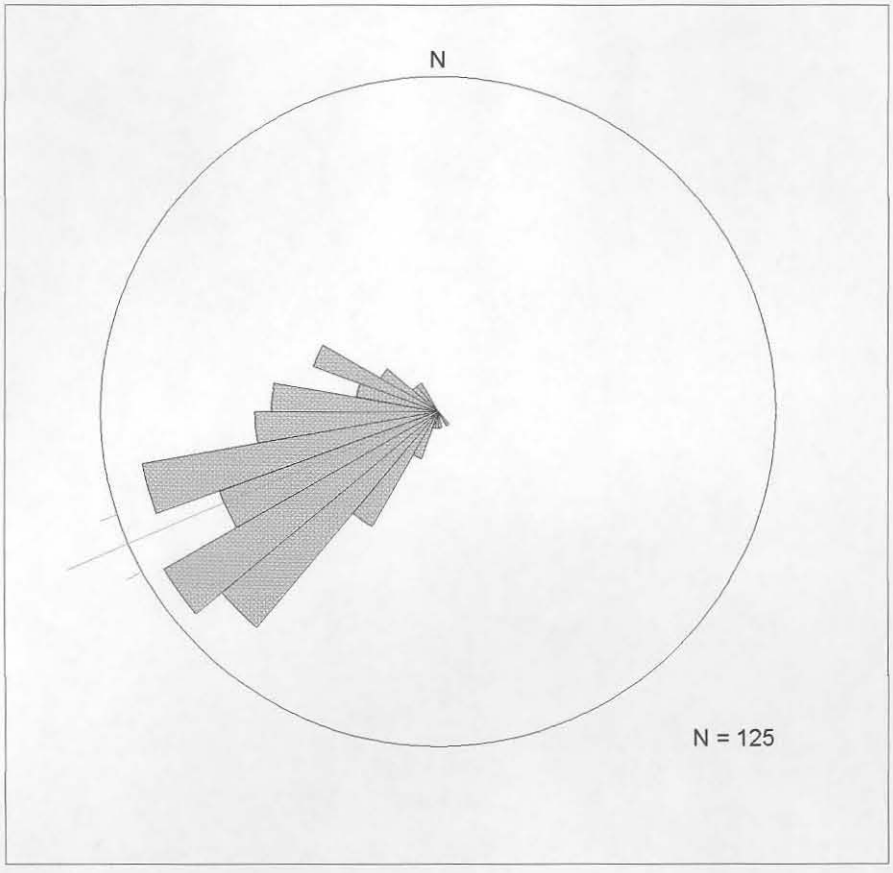

Figure 4.55: Rose diagram to show palaeocurrent directions recorded from trough cross-beds in the Mogalakwena Formation south of the southern strand of the Melinda Fault, in the eastern part of the study area. Principal direction (vector mean) is shown.

Figure 4.56: Sheet-like architectural elements developed at 23°09.36'S; 28°41.92'E. Note that the strata are considerably less conglomeratic than outcrops of Mogalakwena strata further to the east. Cliff is about 50m high.

Figure 4.57: Conglomerate-filled channel form in the Mogalakwena Formation at 23°15.38'S; 28°42.39'E. Strata are bedded parallel to the channel form. Note that pebble size is generally smaller than outcrops of Mogalakwena Formation in the eastern part of the study area (c.f. Figure 4.41). Hammer is 30 cm long.

Figure 4.58: Small (<10cm) trough cross beds with heavy mineral drapes on foresets, characteristic of sandy sheets in the Mogalakwena Formation in the western part of the study area. Recorded at 23°10.23'S; 28°44.18'E. Hammer is 30cm long.

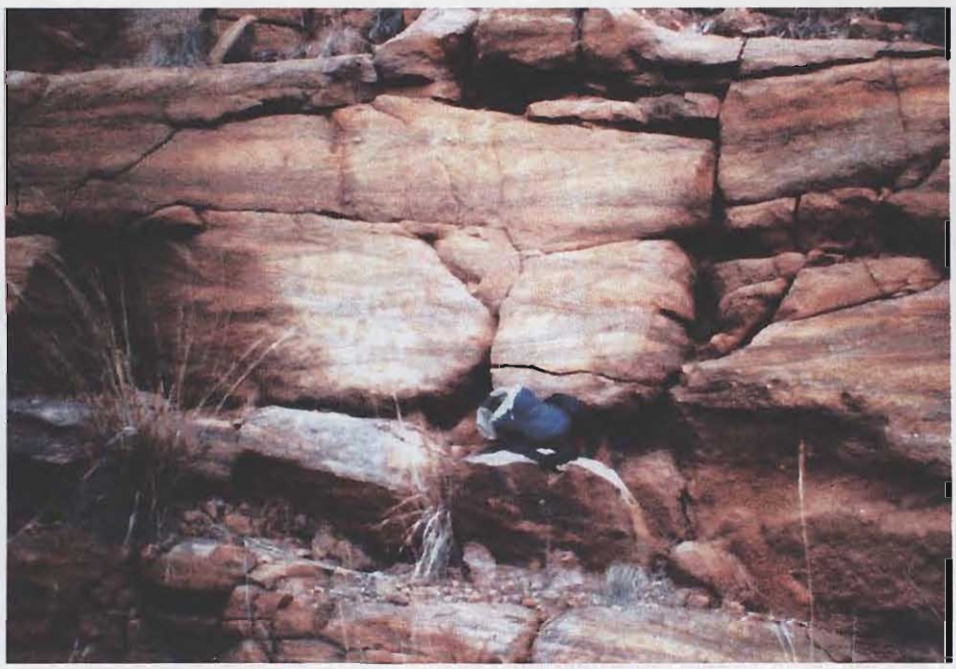

Figure 4.59: Small-scale trough cross-beds developed in the Sandriviersberg Formation (correlated with the Mogalakwena Formation) at 24°20.00'S; 28°33.50'E. Camera bag is 25cm high.

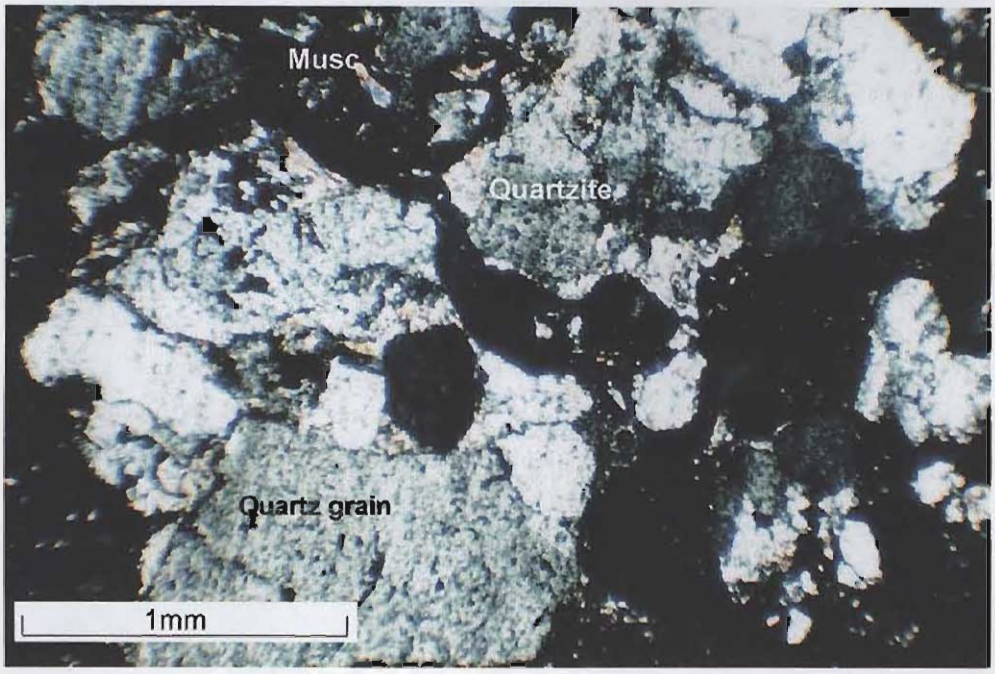

Figure 4.60: Photomicrograph of sandy sheets in the western part of the study area, showing poorly-sorted quartz grains and lithic fragments of quartzite with rare muscovite. Grains are sub-angular with low sphericity.

Figure 4.62: Sheet-like architectural elements of coarse sandstone and granulestone sheets in the Mogalakwena Formation at 23°06'S; 28°54'E. Cliffs are about 200m high.

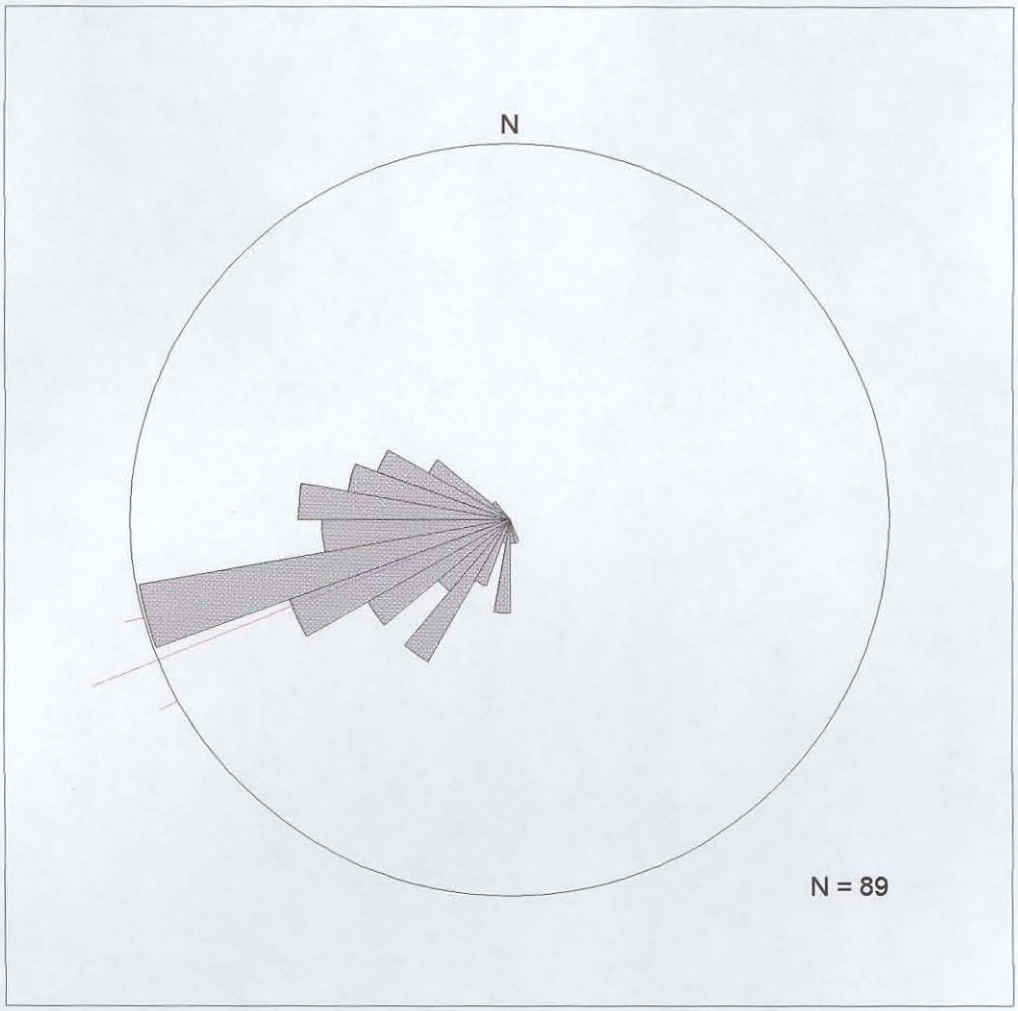

Figure 4.61: Rose diagram showing the palaeocurrent directions recorded from trough cross-beds in the western (distal) outcrops of the Mogalakwena Formation.

Figure 4.63: Thin basal conglomerates of the Mogalakwena Formation at 23°05.76'S; 28°53.47'E. Conglomerates unconformably overlie overturned rocks of the Blouberg Formation (see Chapter 7). Cliff section is 2m high.

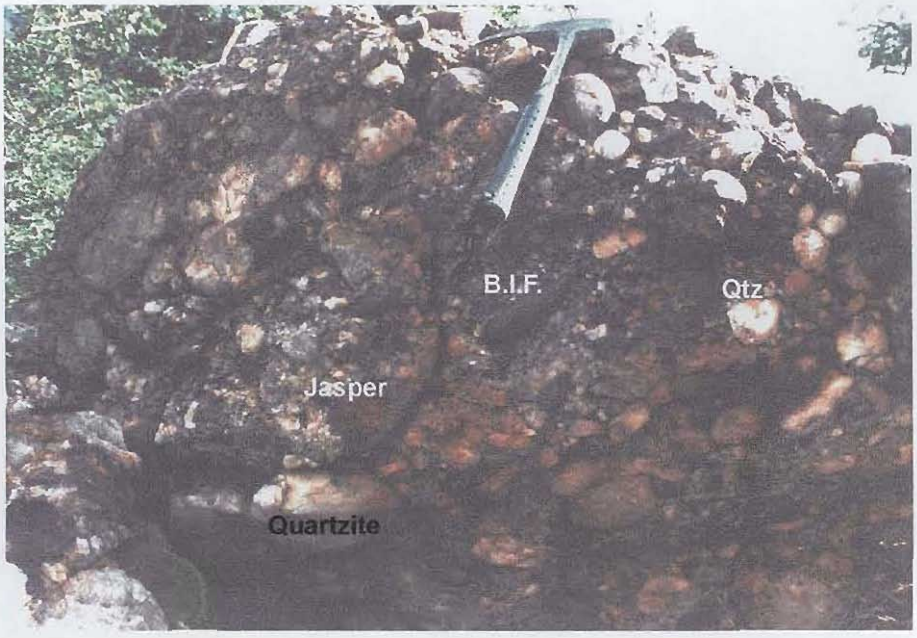

Figure 4.64: Detail of basal conglomerate in the Mogalakwena Formation at 23°05.74'S; 28°53.32'E. Note the presence of quartz, quartzite and B.I.F. clasts (c.f. Figure 4.42) and rare jasper clasts. Hammer is 30cm long.

Figure 4.65: Trough cross-bedded sandstone and granulestone at 23°05.74'S; 28°53.32'E. c.f. Figure 4.43. Pen is 15cm long.

Figure 4.66: Small-scale (<10cm) sets of trough cross-bedded sandstone with heavy mineral drapes developed on foresets. Recorded at 23°07.29'S; 28°57.40'E Note unimodal current direction (towards the W.S.W). c.f. Figure 4.58. Hammer is 30cm long.

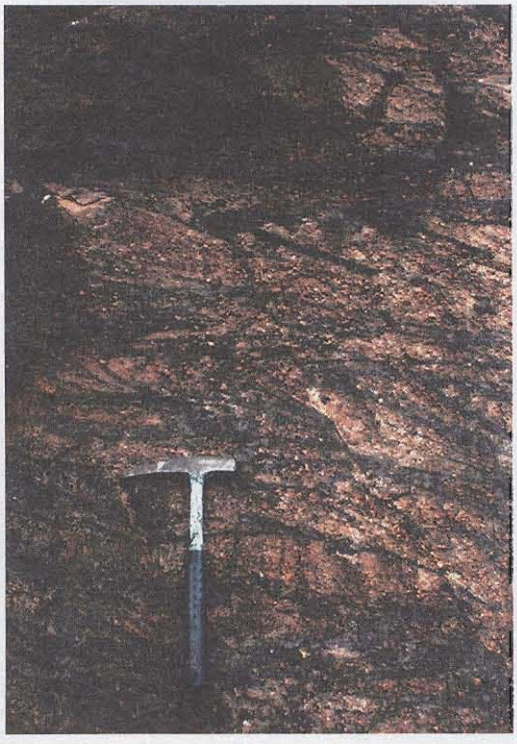

Figure 4.67: Small-scale (< 10cm) sets of trough cross-bedded sandstone with heavy mineral drapes developed on foresets. Recorded at 23° 05.76'S; 28°53.47'E. Hammer is 30cm long.

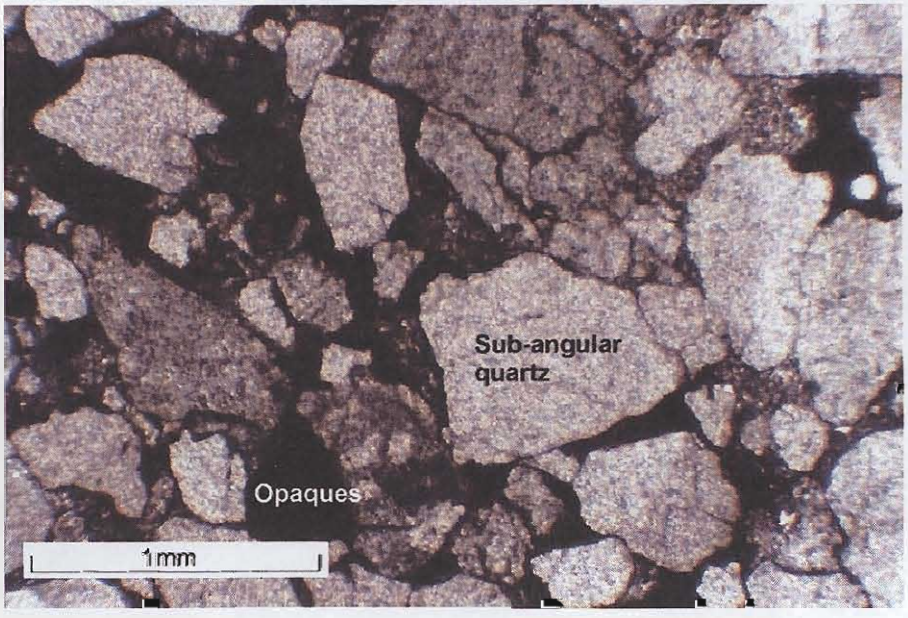

Figure 4.68: Photomicrograph of Mogalakwena strata from 23°05.76'S; 28°53.47'E with sub-angluar quartz grains and high percentage of opaque minerals. (Taken in plane polarised light.)

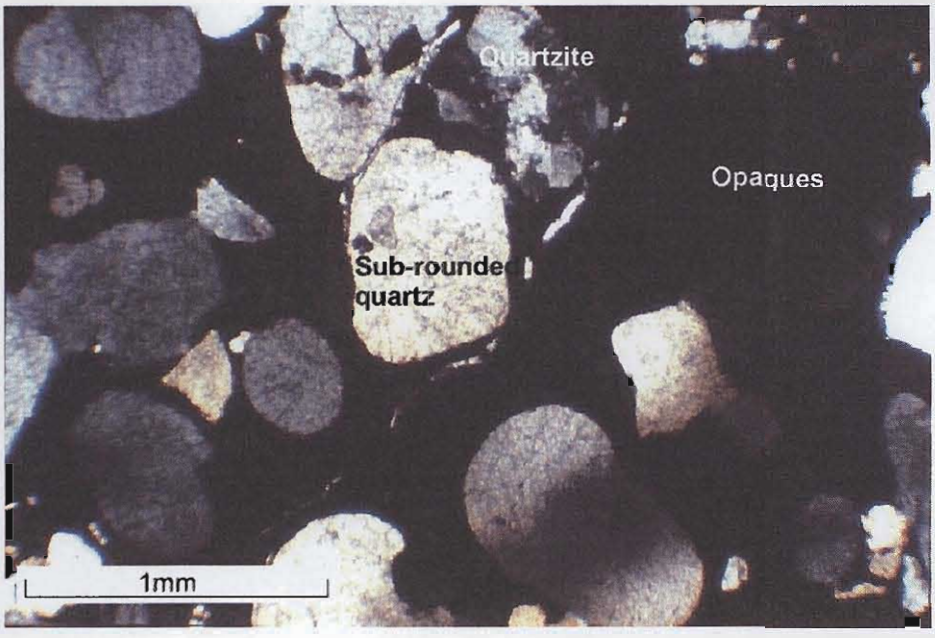

Figure 4.69: Photomicrograph of a thin section of Mogalakwena strata from 23°07.40'S; 28°56.87'E, with rounded to sub-rounded quartz and quartzite grains and opaque interstitial material.

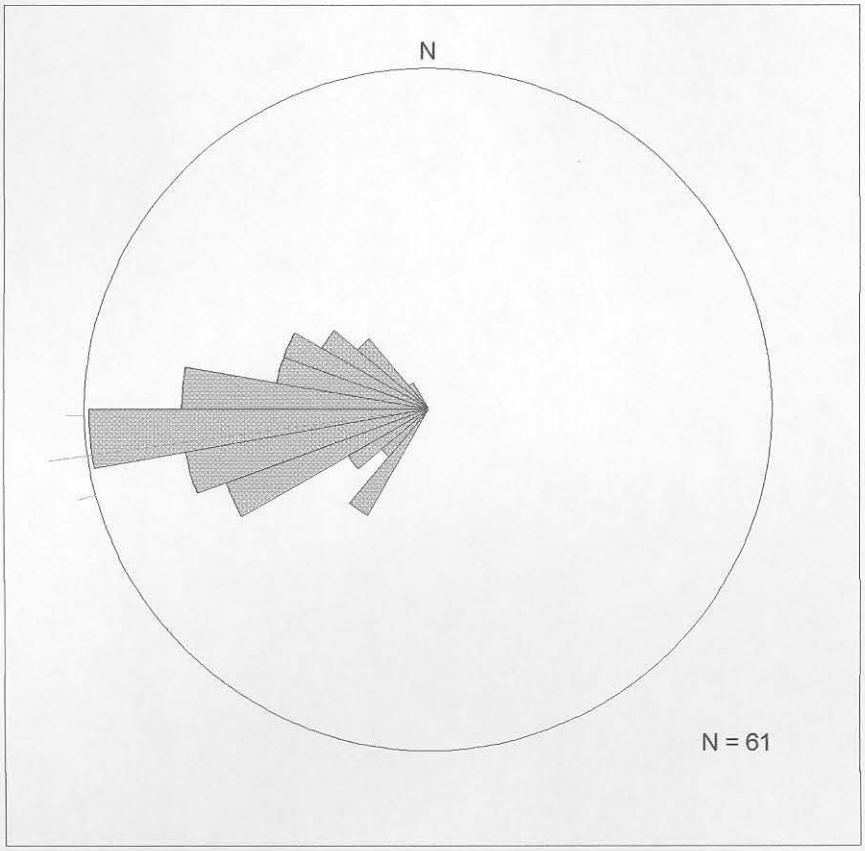

Figure 4.70: Rose diagram showing the palaeocurrent directions recorded from tough cross-beds in the Mogalakwena Formation north of the southern strand of the Melinda Fault. Principal direction (vector mean) is shown.